Search for New Physics with b→sll decays @ LHCb

Simone Bifani
University of Birmingham (UK)
On behalf of the LHCb Collaboration

CERN Seminar, 18th April 2017

A Forward Spectrometer

- Optimized for beauty and charm physics at large pseudorapidity ($2<\eta<5$)
  - **Trigger**: >95% (60-70%) efficient for muons (electrons)
  - **Tracking**: σ_p/p 0.4%–0.6% (p from 5 to 100 GeV), $\sigma_{IP} < 20\ \mu m$
  - **Calorimeter**: $\sigma_E/E \sim 10\% / \sqrt{E} \oplus 1\%$
  - **PID**: ~97% μ,e ID for 1–3% $\pi\rightarrow\mu$,e misID

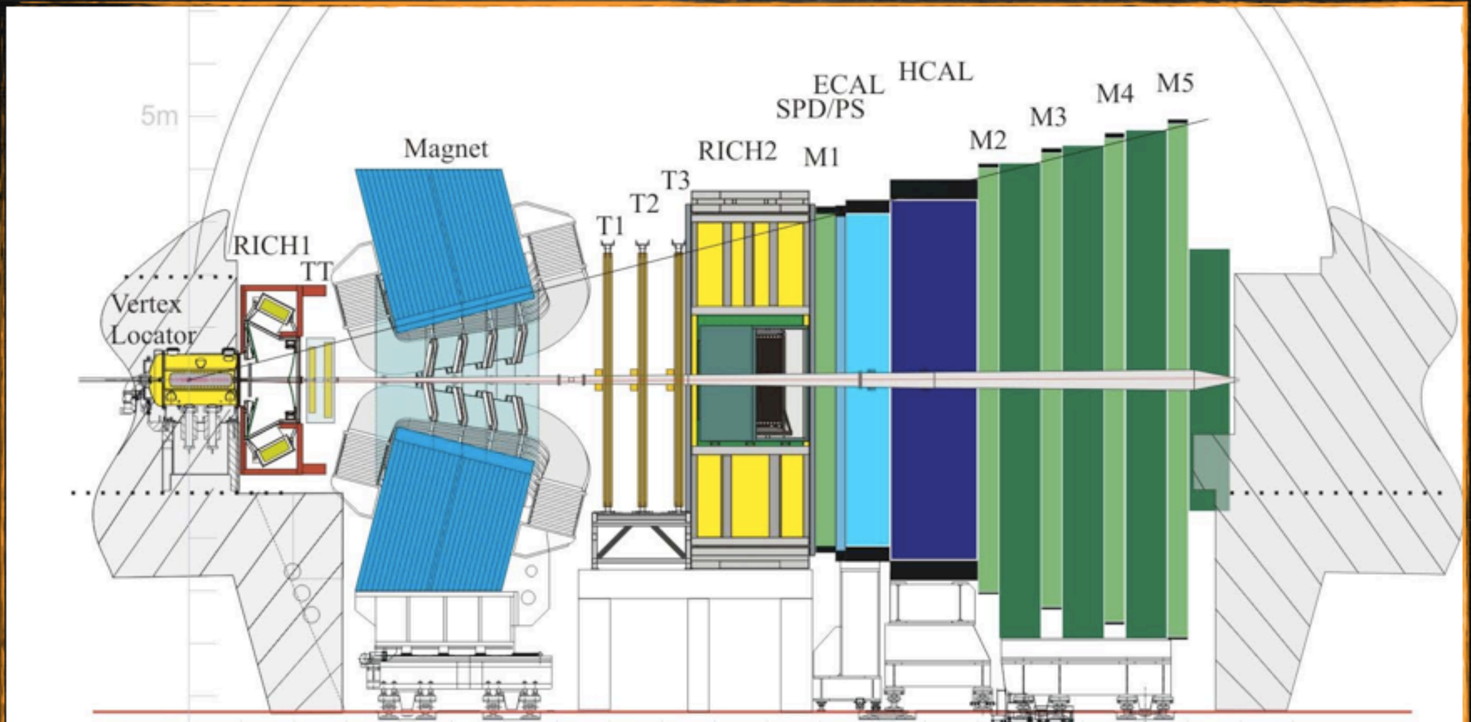

JINST 3 (2008) S08005 Int.J.Mod.Phys. A30 (2015)

Datasets

› Analysis presented today based on the full **Run 1** dataset

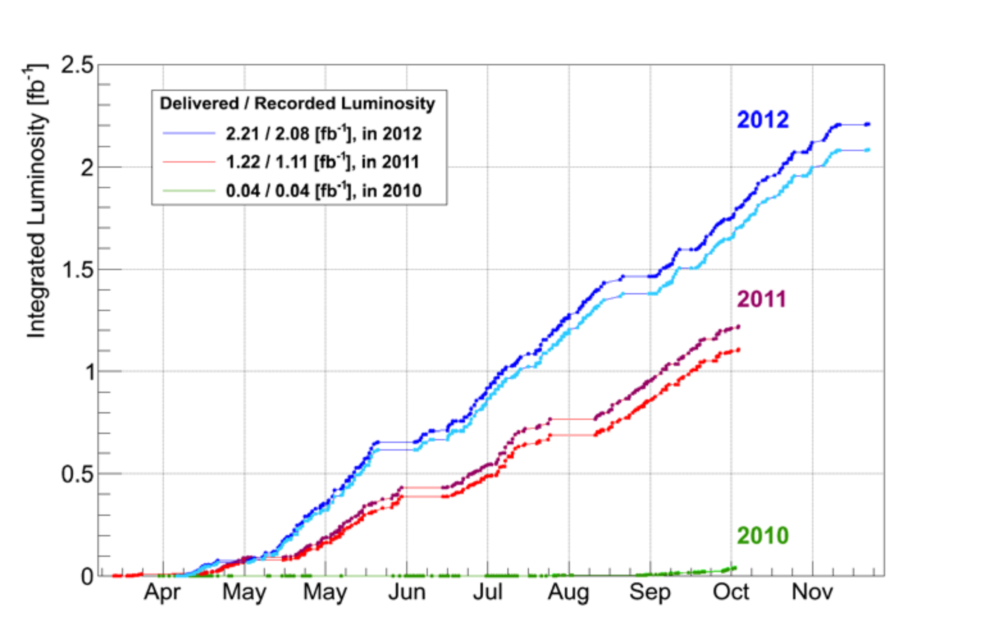

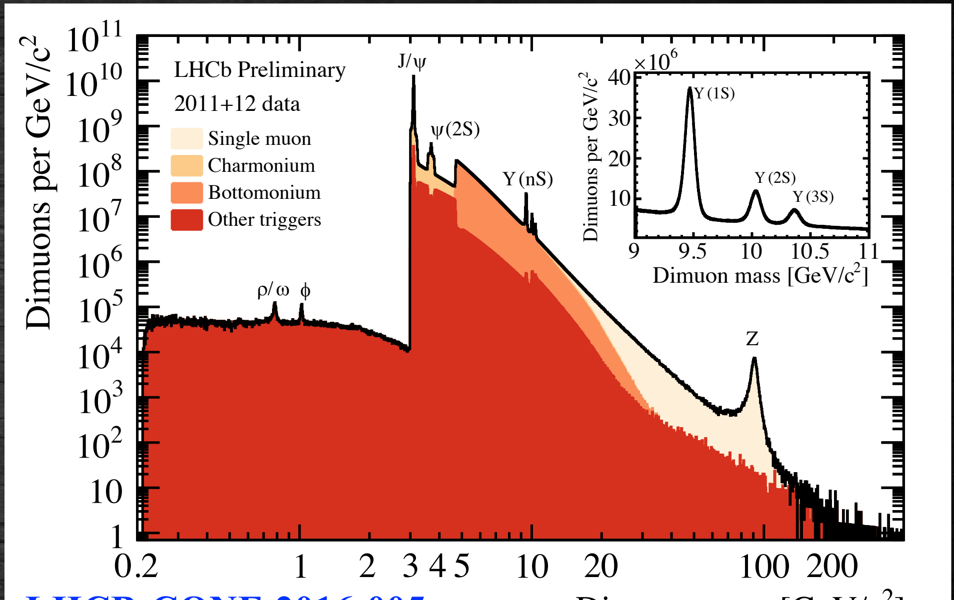

LHCB-CONF-2016-005

› Due to luminosity levelling, same running conditions throughout fills

Why Rare b Decays?

- b→sll decays proceed via **FCNC transitions** that only occur at loop order (or beyond) in the SM

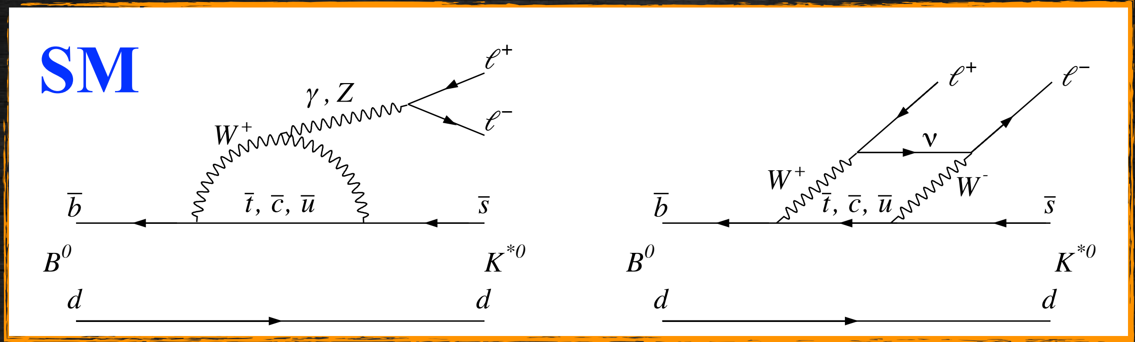

- New particles can for example contribute to loop or tree level diagrams by enhancing/suppressing decay rates, introducing new sources of CP violation or modifying the angular distribution of the final-state particles

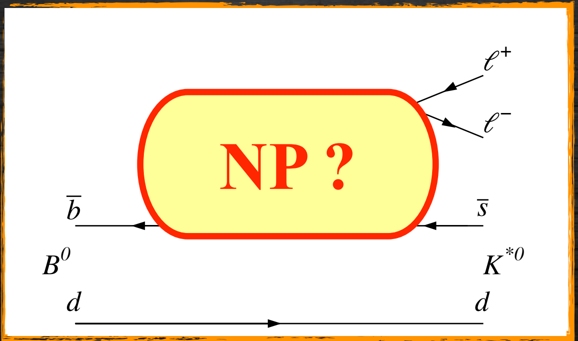

- **Rare b decays place strong constraints on many NP models by probing energy scales higher than direct searches**

Shopping List

- **Differential branching fractions** of $B^0 \to K^{(*)0}\mu\mu$, $B^+ \to K^{(*)+}\mu\mu$, $B_s \to \phi\mu\mu$, $B^+ \to \pi^+\mu\mu$ and $\Lambda_b \to \Lambda\mu\mu$
  - Presence of hadronic uncertainties in theory predictions
- **Angular analyses** of $B \to K^{(*)}\mu\mu$, $B_s \to \phi\mu\mu$, $B^0 \to K^{*0}ee$ and $\Lambda_b \to \Lambda\mu\mu$
  - Define observables with smaller theory uncertainties
- **Test of Lepton Flavour Universality** in $B^+ \to K^+ll$ and **$B^0 \to K^{*0}ll$**
  - Cancellation of hadronic uncertainties in theory predictions

TODAY!

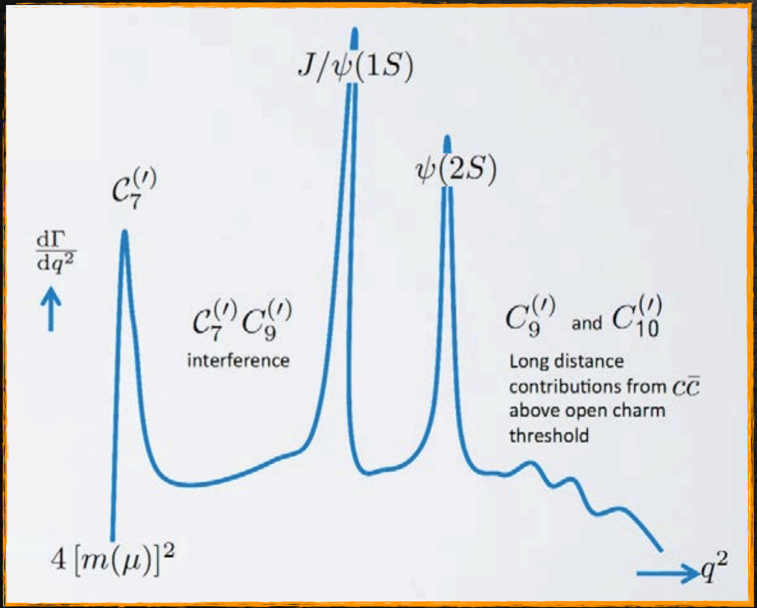

Different q^2 regions probe different processes
In the OPE framework the short-distance contribution is described by Wilson coefficients

$$\mathcal{H}_{eff} = \frac{4G_F}{\sqrt{2}} V_{tb} V_{ts}^* \frac{\alpha_e}{4\pi} \sum [C_i \mathcal{O}_i + C_i' \mathcal{O}_i']$$

Differential Branching Fractions

› Results **consistently lower than SM predictions**

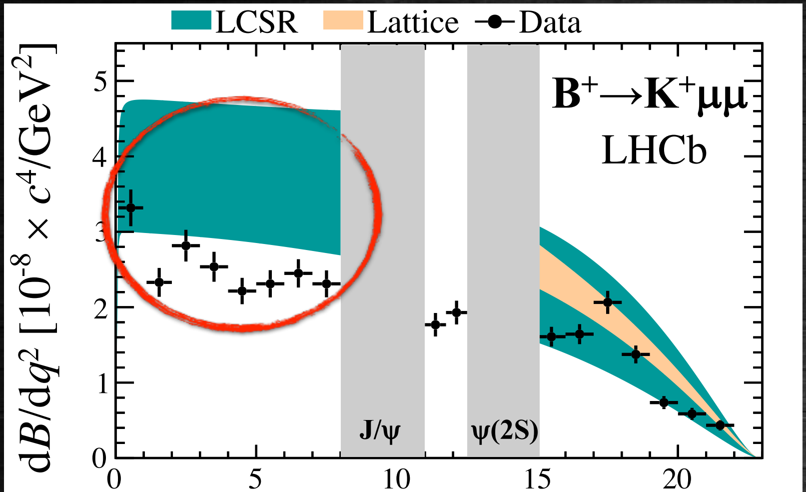

JHEP 06 (2014) 133

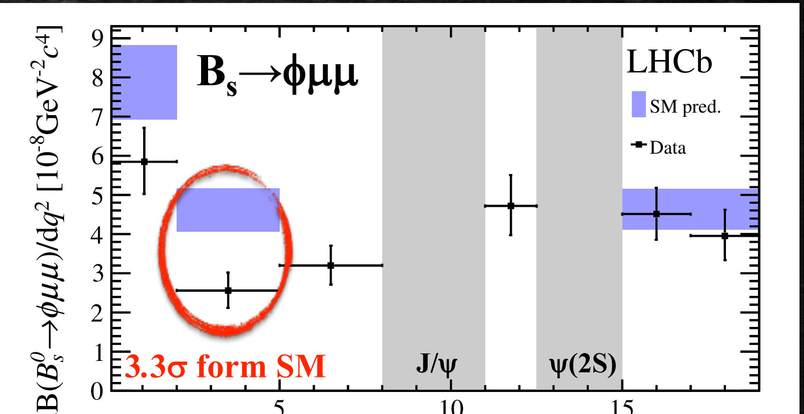

JHEP 09 (2015) 179

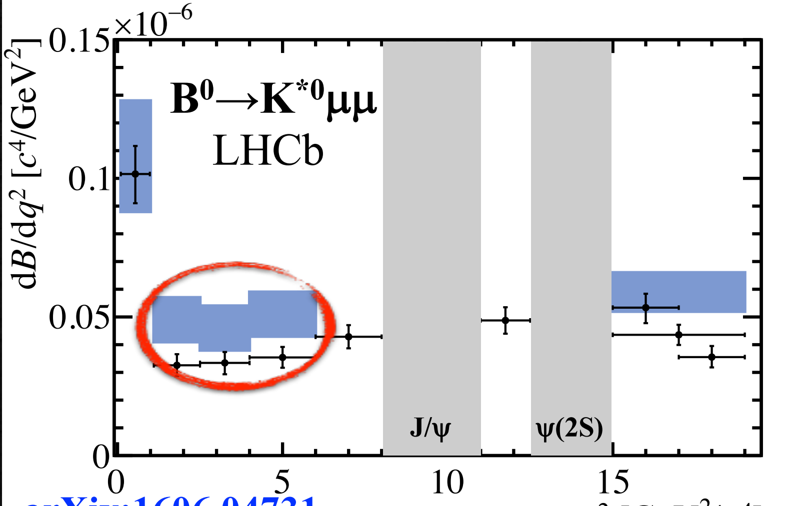

arXiv:1606.04731

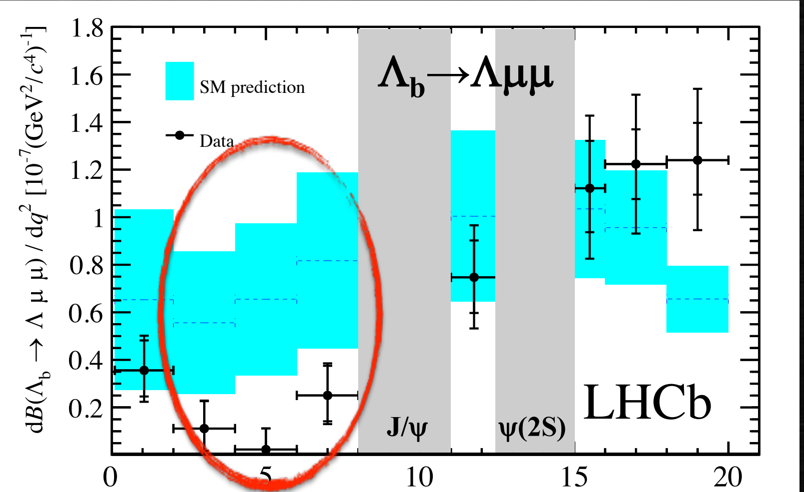

JHEP 06 (2015) 115

Angular Analyses

- First **full angular analysis** of $B^0 \to K^{*0}\mu\mu$: measured all CP-averaged angular terms and CP-asymmetries
- Can construct **less form-factor dependent ratios of observables**

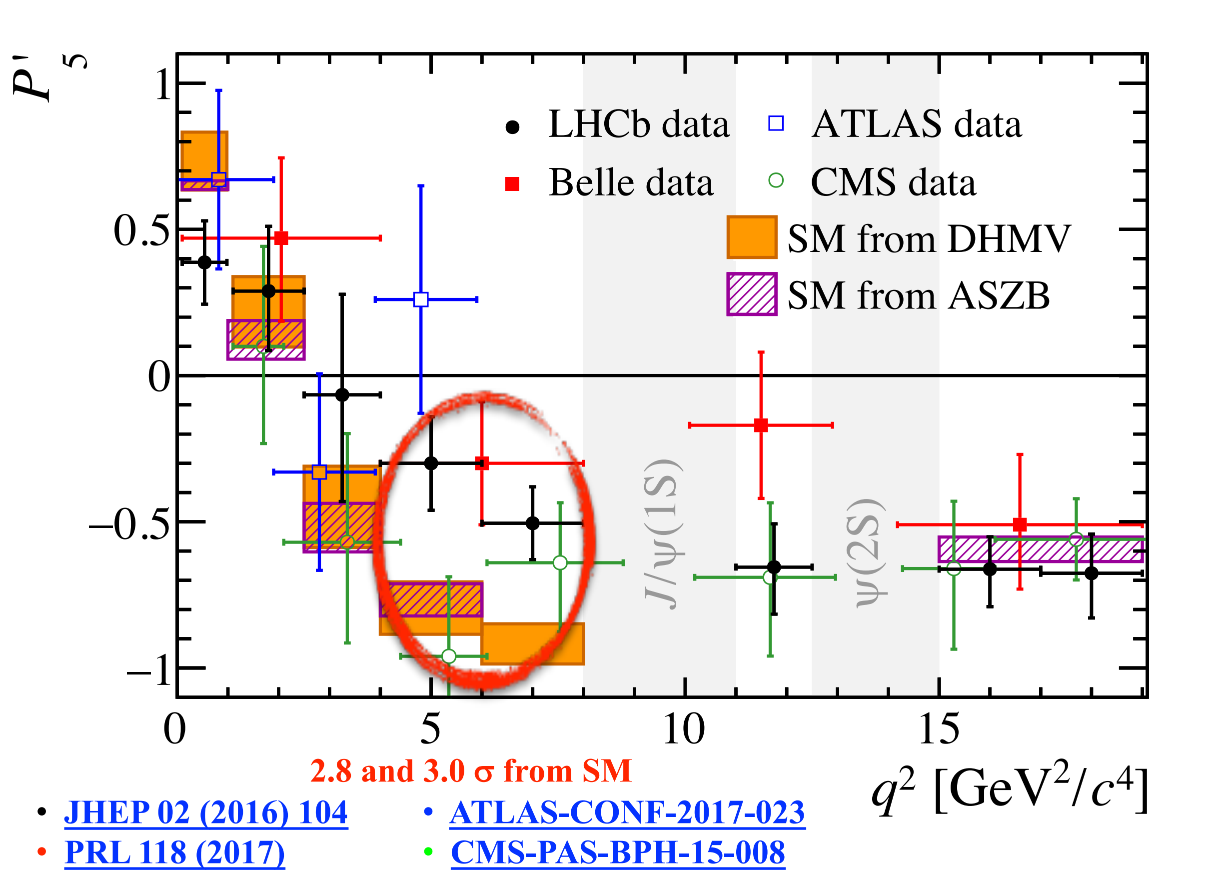

Once upon a time …

- LHCb tested Lepton Universality using **$B^+ \to K^+ ll$** decays and observed a **tension with the SM at 2.6σ**

$$\mathcal{R}_K = \frac{\mathcal{B}(B^+ \to K^+ \mu^+ \mu^-)}{\mathcal{B}(B^+ \to K^+ J/\psi(\to \mu^+ \mu^-))} \Bigg/ \frac{\mathcal{B}(B^+ \to K^+ e^+ e^-)}{\mathcal{B}(B^+ \to K^+ J/\psi(\to e^+ e^-))}$$

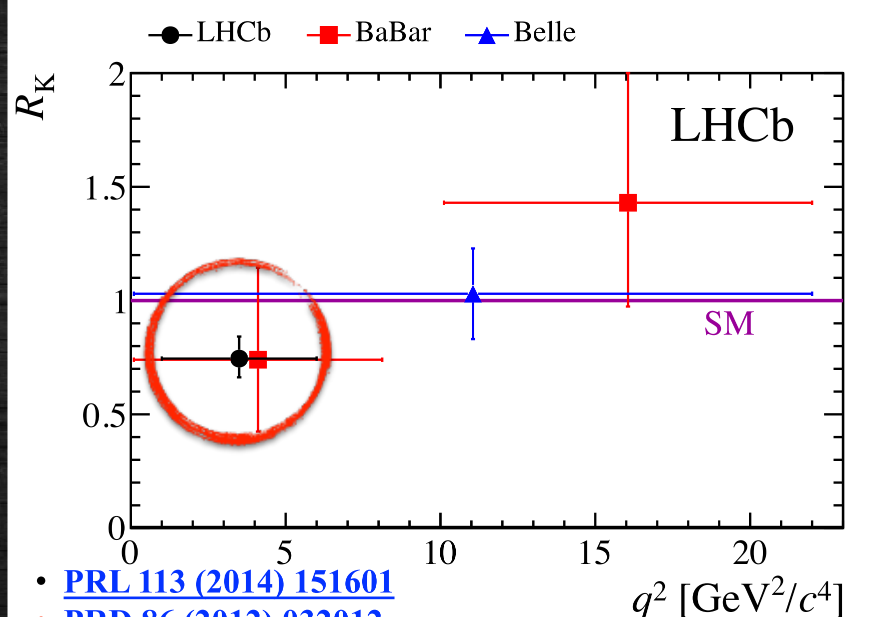

- PRL 113 (2014) 151601
- PRD 86 (2012) 032012
- PRL 103 (2009) 171801

- Consistent with observed BR($B^+ \to K^+ \mu\mu$) if NP does not couple to electrons
- **Observation of LFU violations would be a clear sign of NP**

Global Fits

- Several attempts to interpret results by performing **global fits to data**

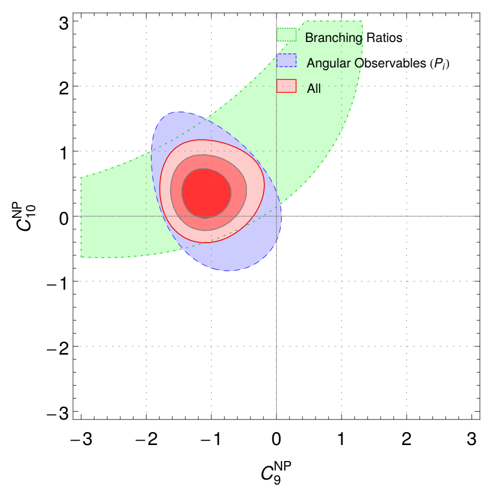

arXiv:1510.04239

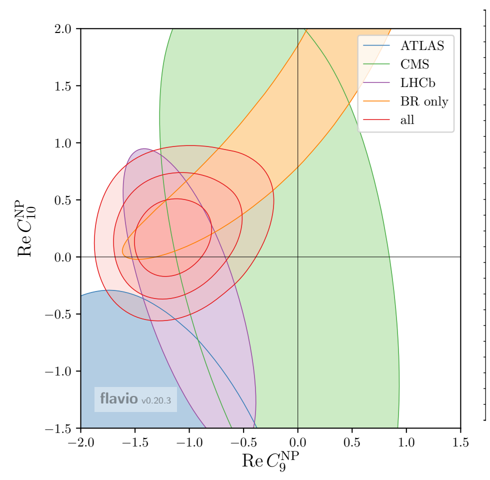

arXiv:1703.09189

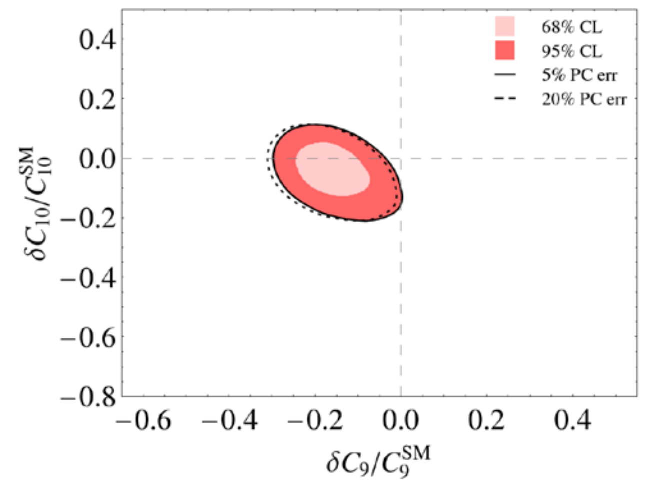

arXiv:1611.05060

- Take into account ~90 observables from different experiments, including $B\to\mu\mu$ and $b\to sll$ transitions
- All global fits require an **additional contribution with respect to the SM to accommodate the data, with a preference for NP in C_9 at ~4σ**
- **Or is this a problem with the understanding of QCD?** (e.g. correctly estimating the contribution from charm loops?)

Today …

› Test of LFU with **$B^0 \to K^{*0}\mu\mu$** and **$B^0 \to K^{*0}ee$, $R_{K^{*0}}$**

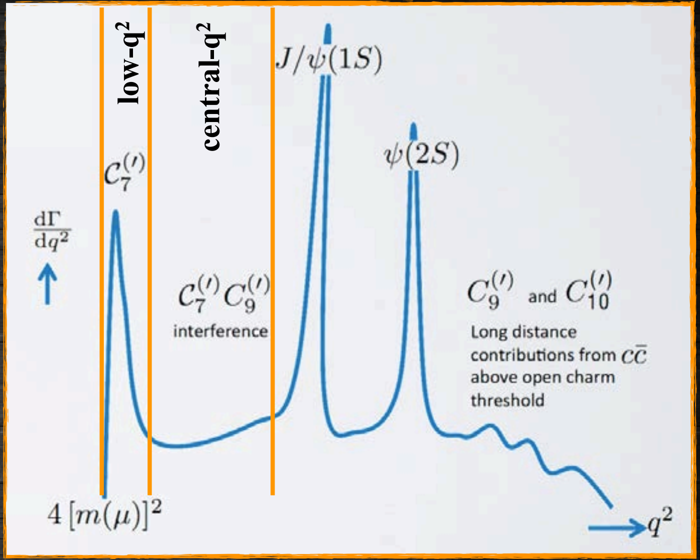

› **Two regions of q²**

- » Low [0.045-1.1] GeV^2/c^4
- » Central [1.1-6.0] GeV^2/c^4

› Measured relative to **$B^0 \to K^{*0}J/\psi(ll)$** in order to reduce systematics

› K^{*0} reconstructed as **$K^+\pi^-$** within 100MeV from the $K^*(892)^0$

› **Blind analysis** to avoid experimental biases

› Extremely challenging due to significant differences in the way μ and e "interact" with the detector

- » Bremsstrahlung
- » Trigger

Bremsstrahlung – I

› Electrons emit a large amount of bremsstrahlung that results in degraded momentum and mass resolutions

› **Two types of bremsstrahlung**

» **Downstream of the magnet**

- photon energy in the same calorimeter cell as the electron
- momentum correctly measured

» **Upstream of the magnet**

- photon energy in different calorimeter cells than electron
- momentum evaluated after bremsstrahlung

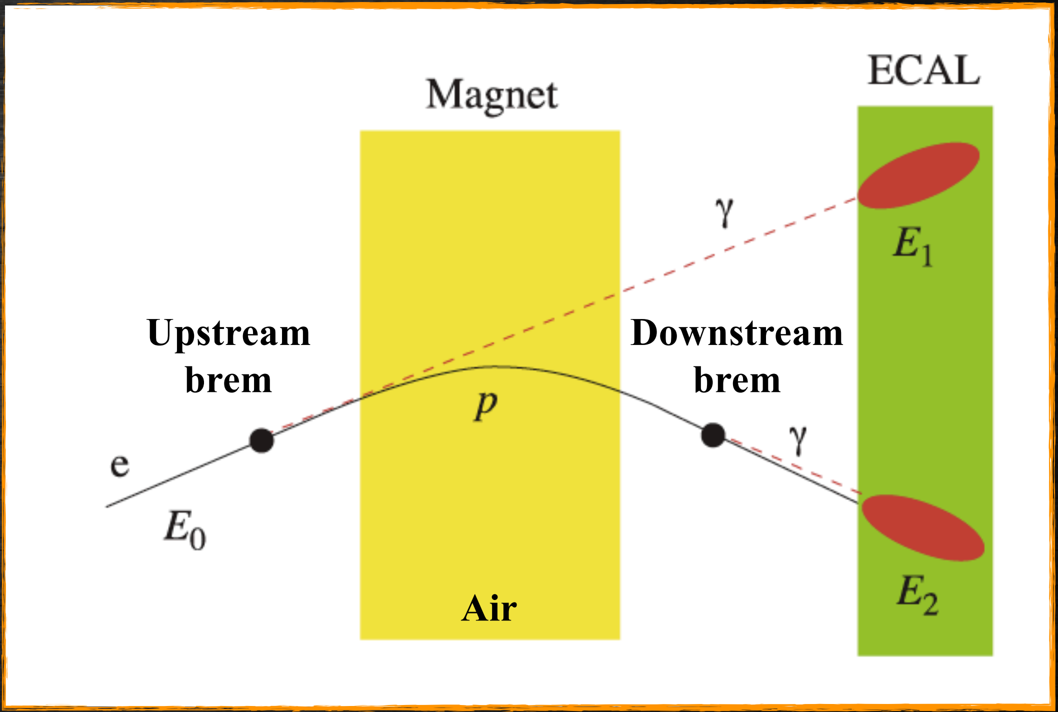

Bremsstrahlung – II

- A **recovery procedure** is in place to improve the momentum reconstruction
- Events are categorised depending on the number of recovered photon clusters
- Incomplete recovery due to
  - Energy threshold of the bremsstrahlung photon ($E_T > 75$ MeV)
  - Calorimeter acceptance
  - Presence of energy deposits mistaken as bremsstrahlung photons

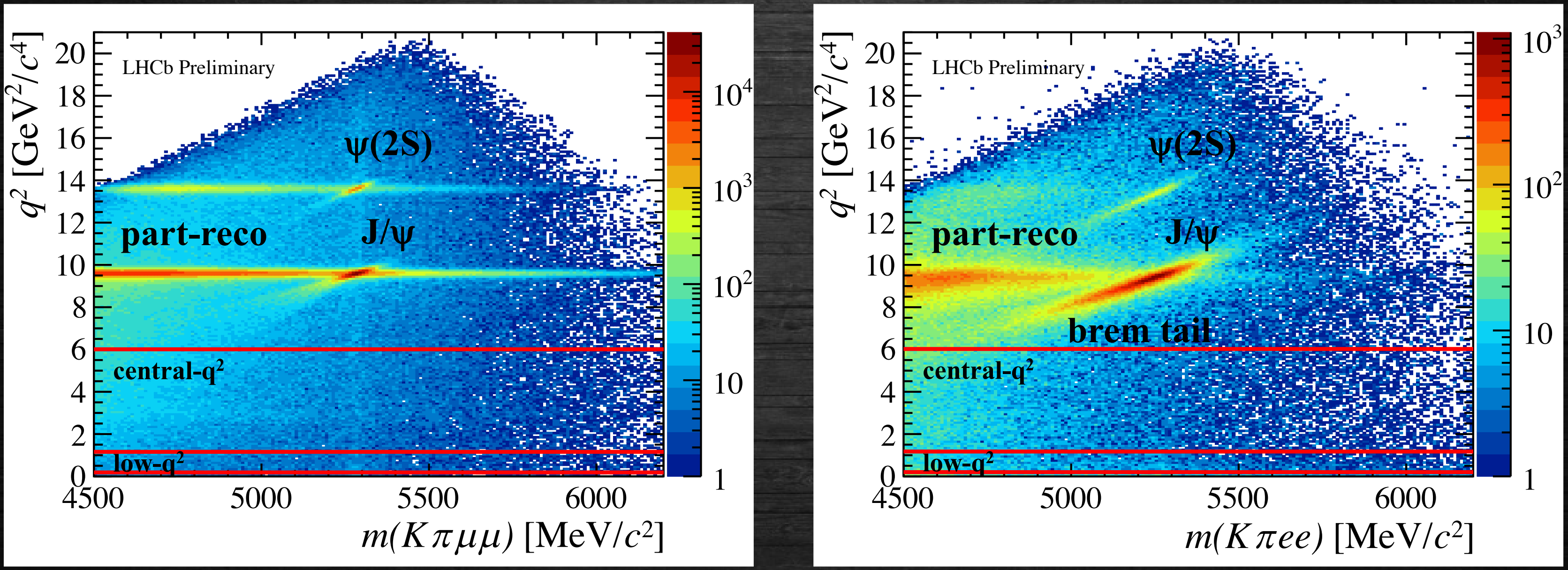

- Incomplete recovery causes the reconstructed B mass to shift towards lower values and events to migrate in and out of the q^2 bins

Trigger

- Trigger system split in hardware (L0) and software (HLT) stages
- Due to higher occupancy of the calorimeters compared to the muon stations, hardware thresholds on the electron E_T are higher than on the muon p_T (**L0 Muon**, p_T>1.5,1.8 GeV)
- To partially mitigate this effect, **3 exclusive trigger categories** are defined
  - **L0 Electron**: electron hardware trigger fired by clusters associated to at least one of the two electrons (E_T > 2.5 GeV)
  - **L0 Hadron**: hadron hardware trigger fired by clusters associated to at least one of the K^{*0} decay products (E_T > 3.5 GeV)
  - **L0 TIS**: any hardware trigger fired by particles in the event not associated to the signal candidate

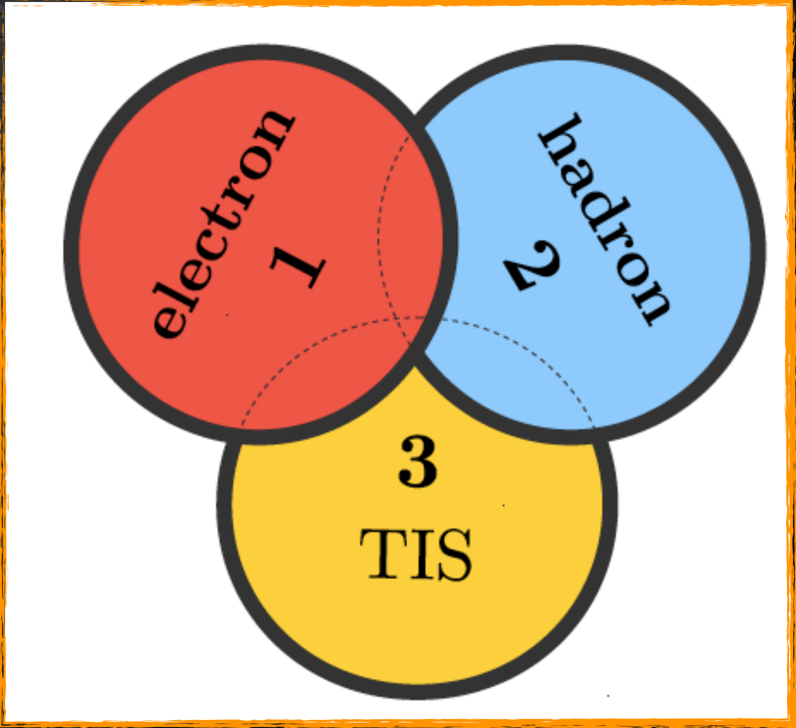

Strategy

› $R_{K^{*0}}$ determined as double ratio to reduce systematic effects

$$\mathcal{R}_{K^{*0}} = \frac{\mathcal{B}(B^0 \to K^{*0}\mu^+\mu^-)}{\mathcal{B}(B^0 \to K^{*0}J/\psi(\to \mu^+\mu^-))} \bigg/ \frac{\mathcal{B}(B^0 \to K^{*0}e^+e^-)}{\mathcal{B}(B^0 \to K^{*0}J/\psi(\to e^+e^-))}$$

› **Selection as similar as possible between μμ and ee**

» Pre-selection requirements on trigger and quality of the candidates

» Cuts to remove the peaking backgrounds

» Particle identification to further reduce the background

» Multivariate classifier to reject the combinatorial background

» Kinematic requirements to reduce the partially-reconstructed backgrounds

» Multiple candidates randomly rejected (1-2%)

› **Efficiencies**

» Determined using simulation, but tuned using data

Corrections to Simulation

› Four-step procedure largely based on tag-and-probe technique

1. **Particle identification**
   » PID response of each particle species tuned using dedicated calibration samples

2. **Generator**
   » Event multiplicity and B^0 kinematics matched to data using $B^0 \to K^{*0} J/\psi(\mu\mu)$ decay

3. **Trigger**
   » Hardware and software trigger responses tuned using $B^0 \to K^{*0} J/\psi(ll)$ decays

4. **Data/MC differences**
   » Residual discrepancies in variables entering the MVA reduced using $B^0 \to K^{*0} J/\psi(ll)$ decays

› After tuning, very good data/MC agreement in all key observables

Fit Procedure – μμ

› Fit signal MC to extract initial parameters

› Simultaneous fit to resonant and non-resonant data allowing (some) parameters to vary

› **Signal**

» Hypatia [NIM A, 764, 150 (2014)]

» Free parameters mass shift and width scale

› **Backgrounds**

» **Combinatorial** exponential

» $\Lambda_b \to pK^- J/\psi(\mu\mu)$ simulation & data

» $B_s \to K^{*0} J/\psi(\mu\mu)$ same as signal but shifted by m_{Bs}-m_{B0}

} $B^0 \to K^{*0} J/\psi$ only

Fit Results – μμ

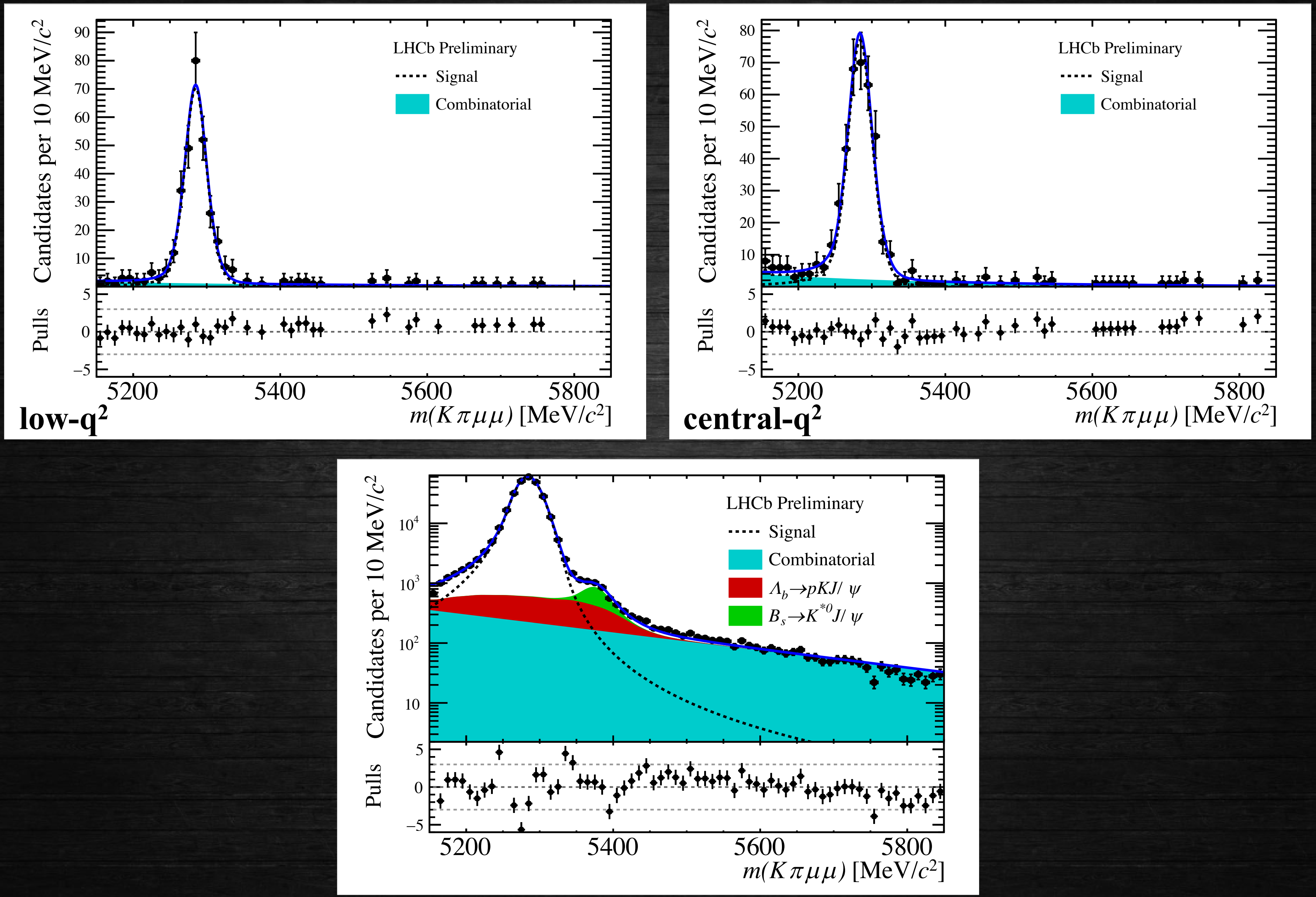

Fit Procedure – ee

- Fit signal MC to extract initial parameters
- Simultaneous fit to resonant and non-resonant data split in trigger categories allowing (some) parameters to vary (bremsstrahlung fractions fixed from MC)

- **Signal**
  - Crystal-Ball (Crystal-Ball and Gaussian)
  - Free parameters — mass shift and width scale

- **Backgrounds**
  - **Combinatorial** — exponential
  - **$\Lambda_b \to pK^- J/\psi(ee)$** — simulation & data, constrained using muons
  - **$B_s \to K^{*0} J/\psi(ee)$** — same as signal but shifted by m_{Bs}-m_{B0}, constrained using muons

  (Λ_b and B_s backgrounds: $B^0 \to K^{*0} J/\psi$ only)

  - **$B^0 \to K^{*0} J/\psi$ Leakage** — simulation, yield constrained using data
  - **Part-Reco** — simulation & data

  (Leakage and Part-Reco: $B^0 \to K^{*0} ee$ only)

Part-Reco Background – I

- Partially-reconstructed backgrounds arise from decays involving **higher K resonances** with one or more decay products in addition to a $K\pi$ pair that are not reconstructed
- Large variety of decays, most abundant due to **$B \to K_1(1270)ee$** and **$B \to K_2^*(1430)ee$**

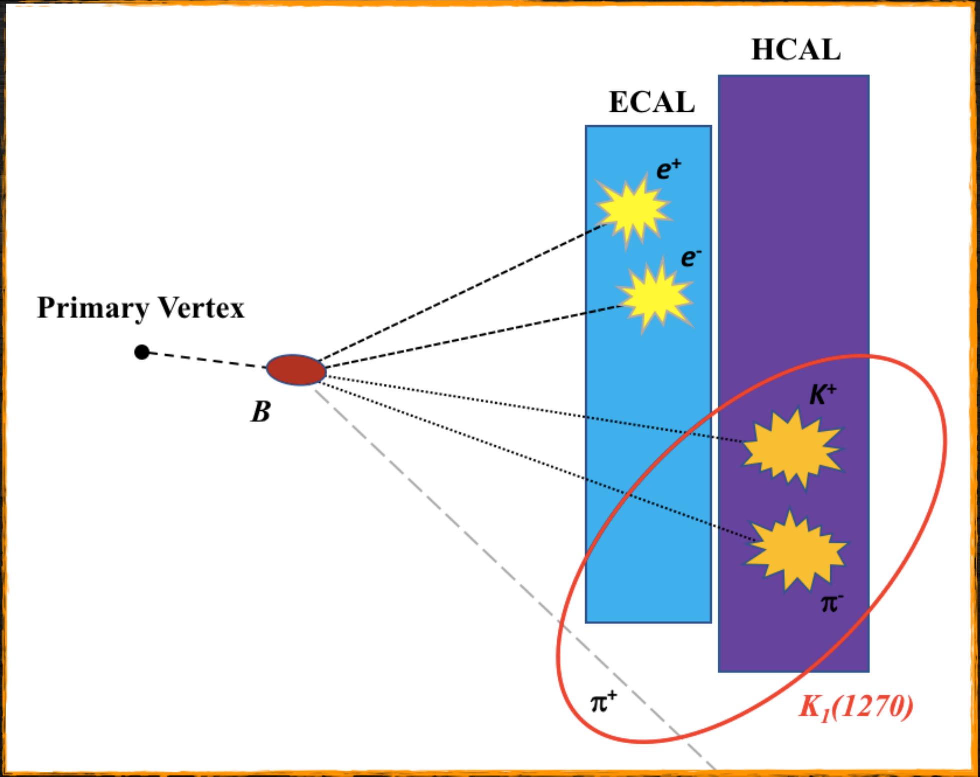

Part-Reco Background – II

› Modelled using two independent methods

» Create a K_1+K_2 cocktail from simulation and use $B \rightarrow XJ/\psi(ee)$ data to determine their relative fraction

» Re-weight $B^+ \rightarrow K^+\pi^+\pi^- ee$ simulated events using background subtracted $B^+ \rightarrow K^+\pi^+\pi^-\mu\mu$ data

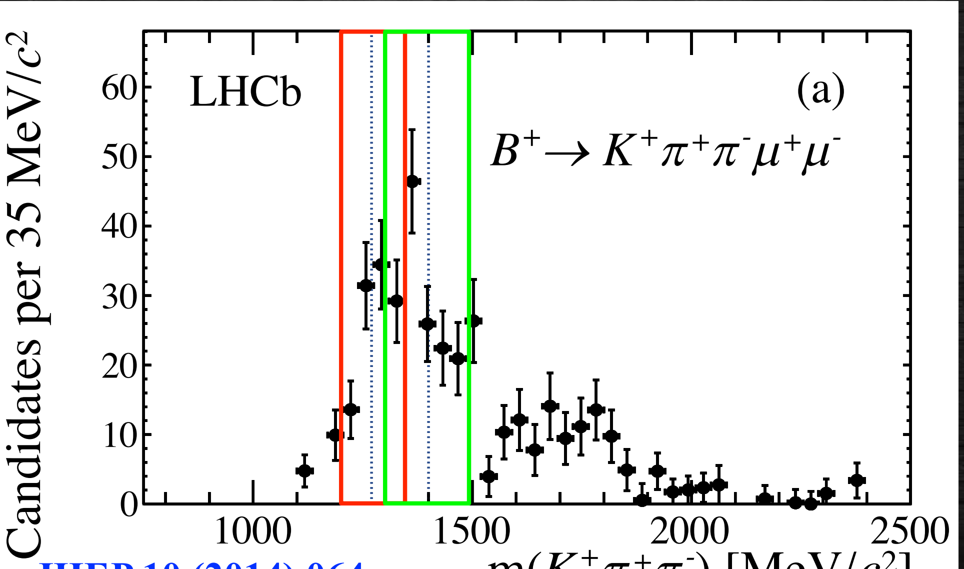

JHEP 10 (2014) 064

Fit Results – ee

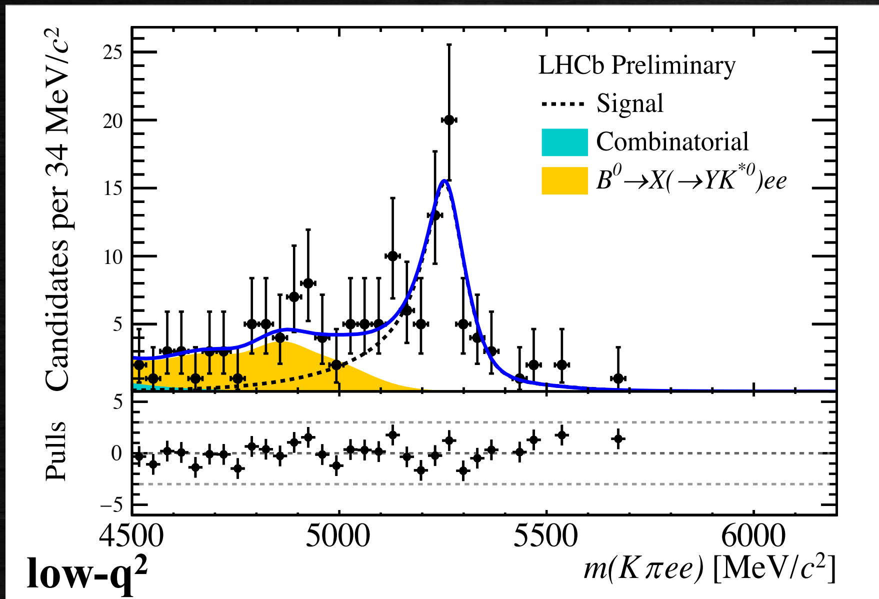

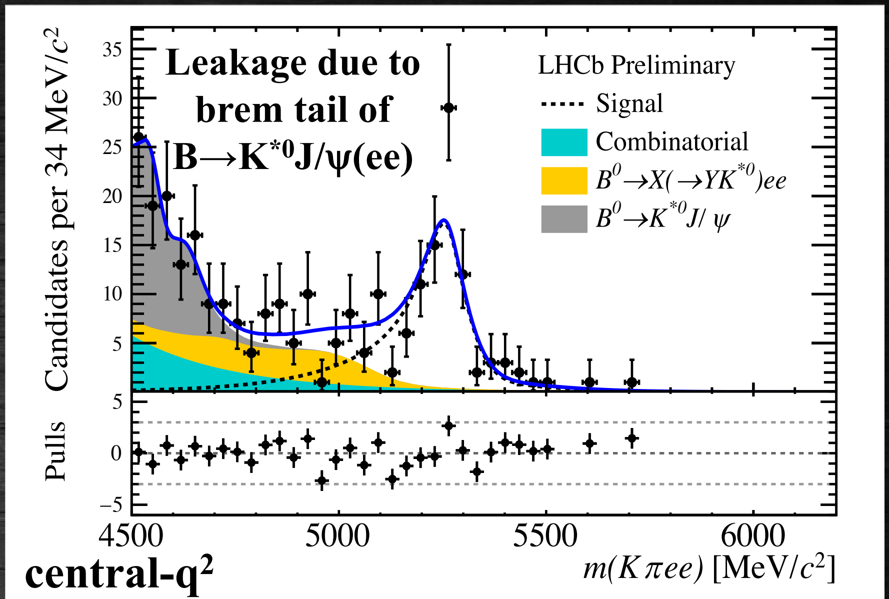

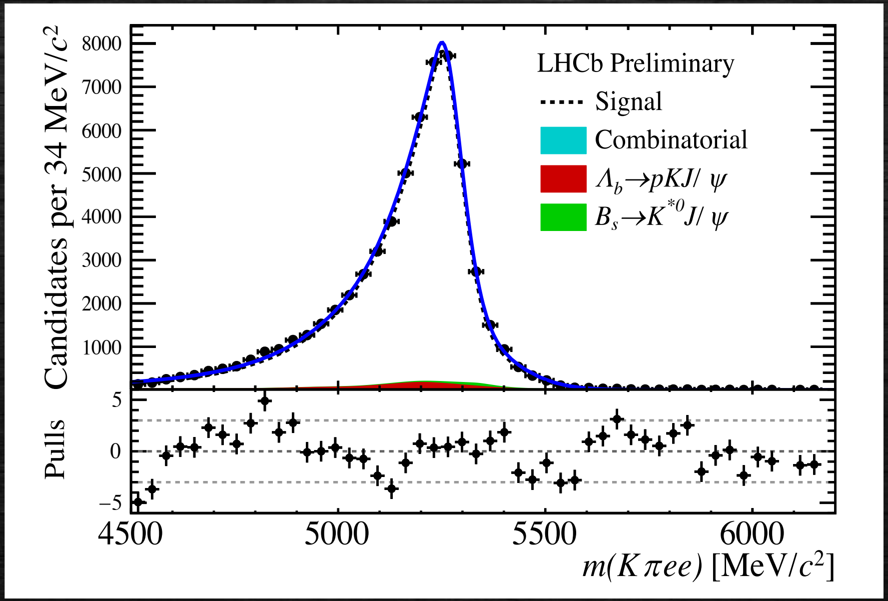

Yields

› Precision of the measurement driven by the statistics of the electron samples

	$B^0 \to K^{*0}\ell^+\ell^-$		$B^0 \to K^{*0}J/\psi(\to \ell^+\ell^-)$
	low-q^2	central-q^2	
$\mu^+\mu^-$	$285 \,^{+\,18}_{-\,18}$	$353 \,^{+\,21}_{-\,21}$	$274416 \,^{+\,602}_{-\,654}$
e^+e^- (L0E)	$55 \,^{+\,9}_{-\,8}$	$67 \,^{+\,10}_{-\,10}$	$43468 \,^{+\,222}_{-\,221}$
e^+e^- (L0H)	$13 \,^{+\,5}_{-\,5}$	$19 \,^{+\,6}_{-\,5}$	$3388 \,^{+\,62}_{-\,61}$
e^+e^- (L0I)	$21 \,^{+\,5}_{-\,4}$	$25 \,^{+\,7}_{-\,6}$	$11505 \,^{+\,115}_{-\,114}$

› In total, about 90 and 110 $B^0 \to K^{*0}ee$ candidates at low- and central-q^2, respectively

Cross-Checks – I

- **Control of the absolute scale of the efficiencies** via the ratio

$$r_{J/\psi} = \frac{\mathcal{B}(B^0 \to K^{*0} J/\psi(\to \mu^+\mu^-))}{\mathcal{B}(B^0 \to K^{*0} J/\psi(\to e^+e^-))}$$

which is expected to be unity and measured to be

$$1.043 \pm 0.006\,(\mathrm{stat}) \pm 0.045\,(\mathrm{syst})$$

- Result observed to be reasonably flat as a function of the decay kinematics and event multiplicity

- Extremely stringent test, which does not benefit from the cancellation of the experimental systematics provided by the double ratio

Cross-Checks – II

- **$BR(B^0 \to K^{*0}\mu\mu)$** in good agreement with [arXiv:1606.04731]

- If **corrections to simulations** are not accounted for, the ratio of the efficiencies changes by less than 5%

- **Further checks** performed by measuring the following ratios

$$\mathcal{R}_{\psi(2S)} = \frac{\mathcal{B}(B^0 \to K^{*0}\psi(2S)(\to \mu^+\mu^-))}{\mathcal{B}(B^0 \to K^{*0}J/\psi(\to \mu^+\mu^-))} \Big/ \frac{\mathcal{B}(B^0 \to K^{*0}\psi(2S)(\to e^+e^-))}{\mathcal{B}(B^0 \to K^{*0}J/\psi(\to e^+e^-))}$$

$$r_\gamma = \frac{\mathcal{B}(B^0 \to K^{*0}\gamma(\to e^+e^-))}{\mathcal{B}(B^0 \to K^{*0}J/\psi(\to e^+e^-))}$$

which are found to be compatible with the expectations

Cross-Checks – III

› Relative population of **bremsstrahlung categories** compared between data and simulation using $B^0 \to K^{*0} J/\psi(ee)$ and $B^0 \to K^{*0}\gamma(ee)$ events

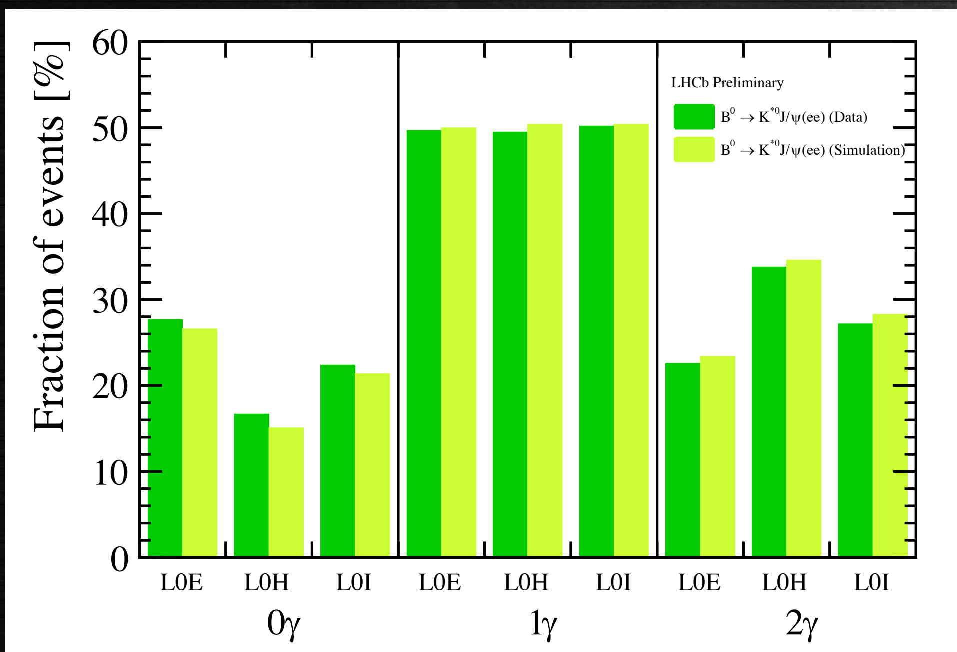

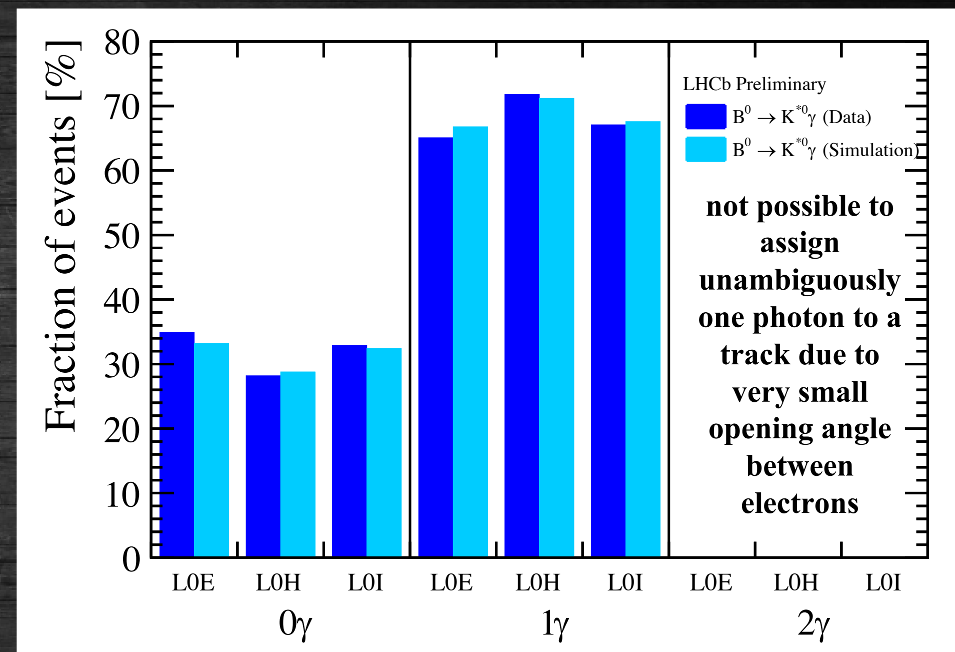

› A good agreement is observed

Cross-Checks – IV

- The sPlot technique is used to statistically subtract the background from the selected data [NIM A555, 356-369 (2005)]

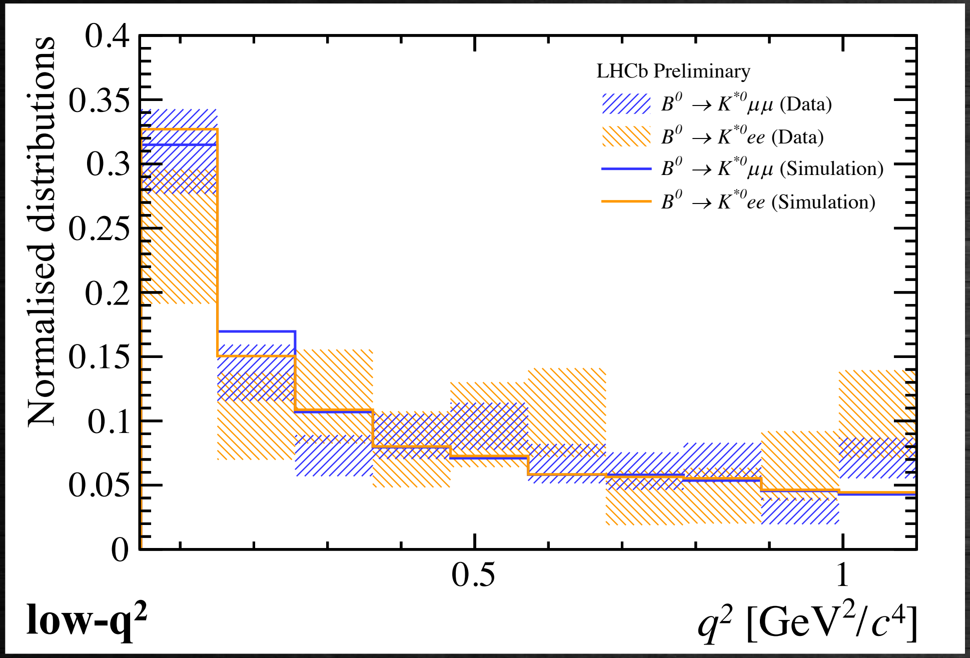

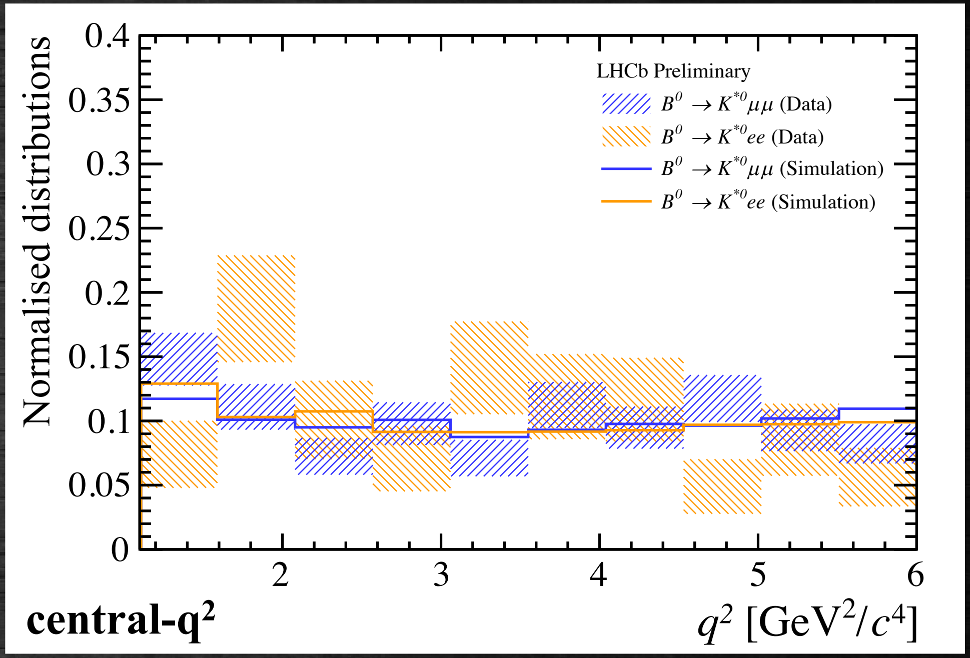

- A good agreement is observed in both q^2 regions between muons and electrons, data and simulation

Cross-Checks – V

› No attempt is made to separate the K^{*0} meson from S-wave or other broad contributions present in the mass peak region

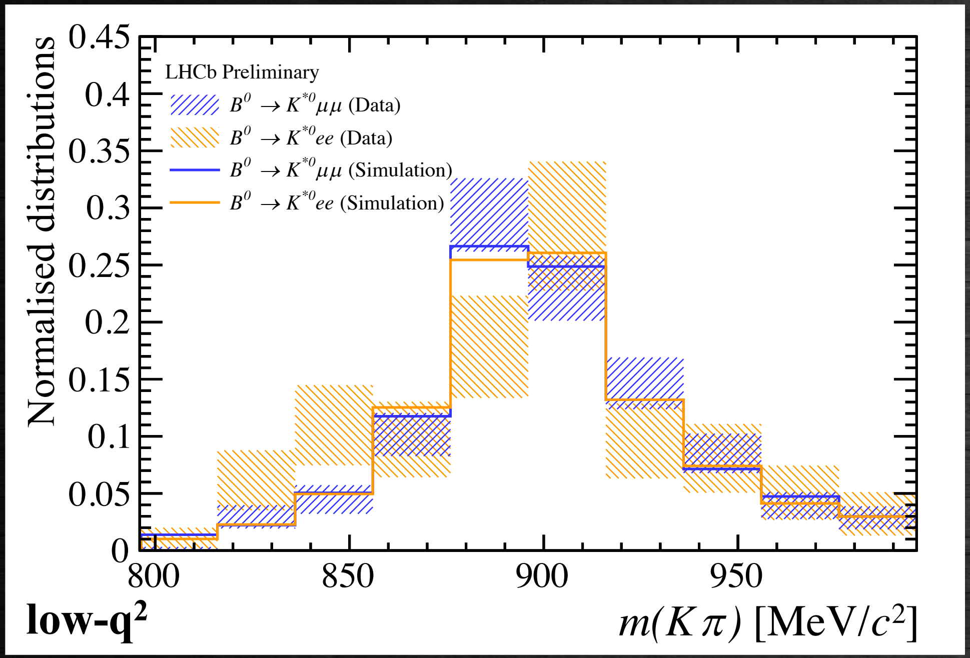

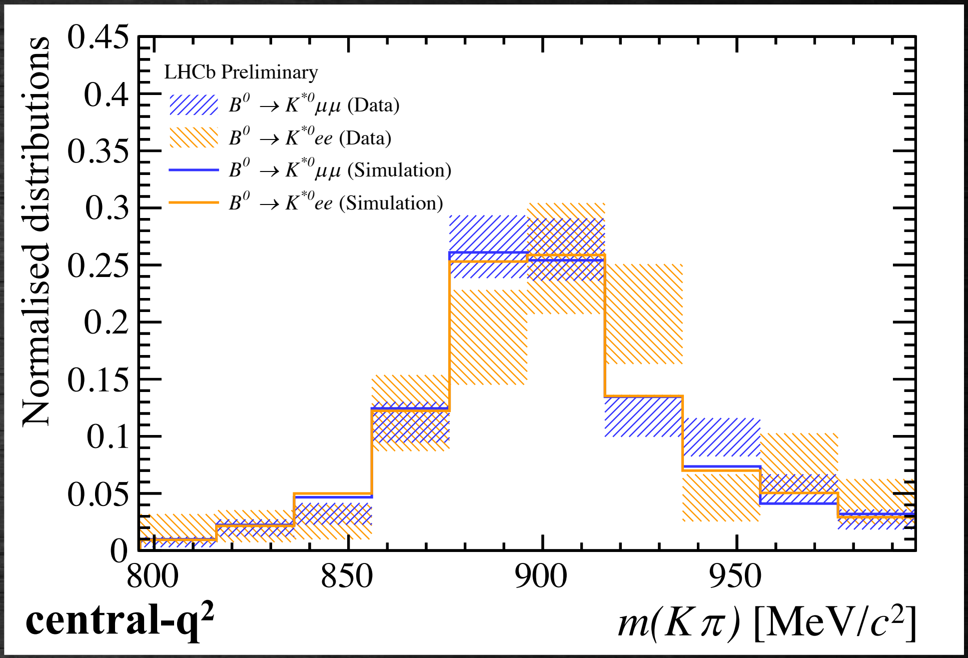

› A clear K^{*0} mass peak is visible, and the muon and electron channels manifest a very good agreement

Cross-Checks – VI

› The opening angle between the two leptons

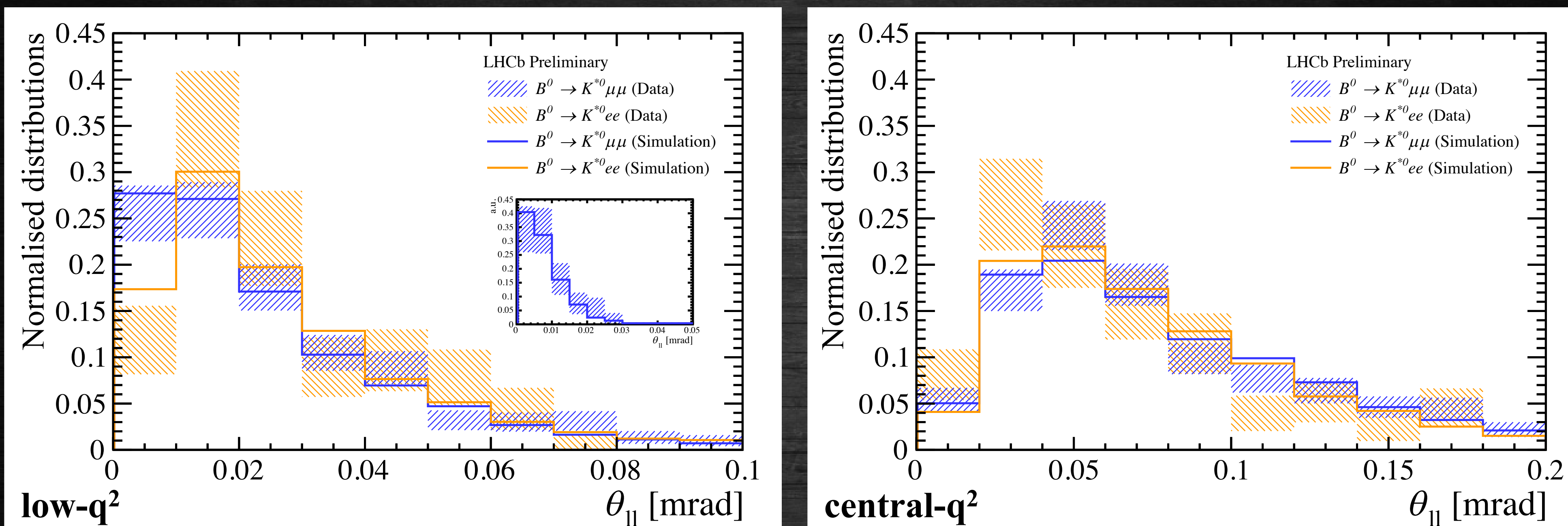

› The distribution is different between muons and electrons at low-q^2 because of the difference in the lepton masses

› Even very close to threshold a good description is observed (insert, $0.045<q^2<0.1$ GeV^2/c^4)

Systematics – I

- $R_{K^{*0}}$ **determined as a double ratio**
  - Many experimental systematic effects cancel
  - Statistically dominated (~15%)

	low-q^2			central-q^2		
Trigger category	L0E	L0H	L0I	L0E	L0H	L0I
Corrections to simulation	2.5	4.8	3.9	2.2	4.2	3.4
Trigger	0.1	1.2	0.1	0.2	0.8	0.2
PID	0.2	0.4	0.3	0.2	1.0	0.5
Kinematic selection	2.1	2.1	2.1	2.1	2.1	2.1
Residual background	–	–	–	5.0	5.0	5.0
Mass fits	1.4	2.1	2.5	2.0	0.9	1.0
Bin migration	1.0	1.0	1.0	1.6	1.6	1.6
$r_{J/\psi}$ flatness	1.6	1.4	1.7	0.7	2.1	0.7
Total	4.0	6.1	5.5	6.4	7.5	6.7

- Total systematic uncertainty of 4-6% and 6-8% in the low- and central-q^2

Systematics – II

- **Corrections to simulation**: besides the uncertainty due to the size of the samples, an additional systematic is determined using different parameterisations of the corrections

- **Kinematic selection**: a systematic uncertainty for Data/MC differences in the description of the bremsstrahlung tail and the MVA classifier is determined by comparing simulation and background subtracted $B^0 \to K^{*0} J/\psi(ll)$ data

- **Residual background**: both data and simulation are used to assess a systematic uncertainty for residual background contamination due to $B^0 \to K^{*0} J/\psi(ee)$ events with a $K \leftrightarrow e$ or $\pi \leftrightarrow e$ swap

	low-q^2			central-q^2		
Trigger category	L0E	L0H	L0I	L0E	L0H	L0I
Corrections to simulation	2.5	4.8	3.9	2.2	4.2	3.4
Trigger	0.1	1.2	0.1	0.2	0.8	0.2
PID	0.2	0.4	0.3	0.2	1.0	0.5
Kinematic selection	2.1	2.1	2.1	2.1	2.1	2.1
Residual background	–	–	–	5.0	5.0	5.0
Mass fits	1.4	2.1	2.5	2.0	0.9	1.0
Bin migration	1.0	1.0	1.0	1.6	1.6	1.6
$r_{J/\psi}$ flatness	1.6	1.4	1.7	0.7	2.1	0.7
Total	4.0	6.1	5.5	6.4	7.5	6.7

Systematics – III

- **Mass fit**: a systematic uncertainty is determined by running pseudo-experiments with different descriptions of the signal and background fit models
- **Bin migration**: the effect of the model dependence and description of the q^2 resolution in simulation are assigned as a systematic uncertainty
- **$r_{J/\psi}$ flatness**: the ratio is studied as a function of several properties of the event and decay products, and the observed residual deviations from unity are used to assign a systematic uncertainty

	low-q^2			central-q^2		
Trigger category	L0E	L0H	L0I	L0E	L0H	L0I
Corrections to simulation	2.5	4.8	3.9	2.2	4.2	3.4
Trigger	0.1	1.2	0.1	0.2	0.8	0.2
PID	0.2	0.4	0.3	0.2	1.0	0.5
Kinematic selection	2.1	2.1	2.1	2.1	2.1	2.1
Residual background	–	–	–	5.0	5.0	5.0
Mass fits	1.4	2.1	2.5	2.0	0.9	1.0
Bin migration	1.0	1.0	1.0	1.6	1.6	1.6
$r_{J/\psi}$ flatness	1.6	1.4	1.7	0.7	2.1	0.7
Total	4.0	6.1	5.5	6.4	7.5	6.7

Results – I

LHCb Preliminary	low-q^2	central-q^2
$\mathcal{R}_{K^{*0}}$	$0.660\ ^{+\ 0.110}_{-\ 0.070} \pm 0.024$	$0.685\ ^{+\ 0.113}_{-\ 0.069} \pm 0.047$
95% CL	[0.517–0.891]	[0.530–0.935]
99.7% CL	[0.454–1.042]	[0.462–1.100]

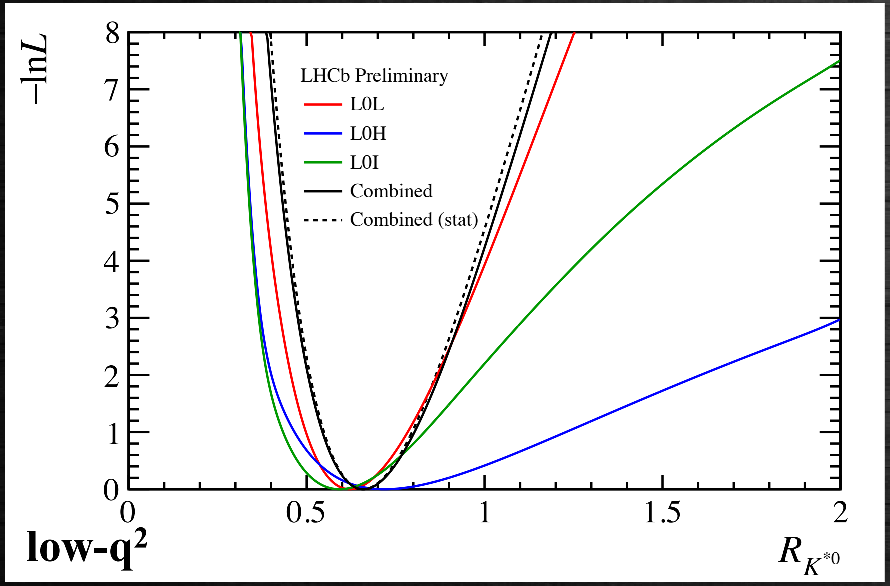

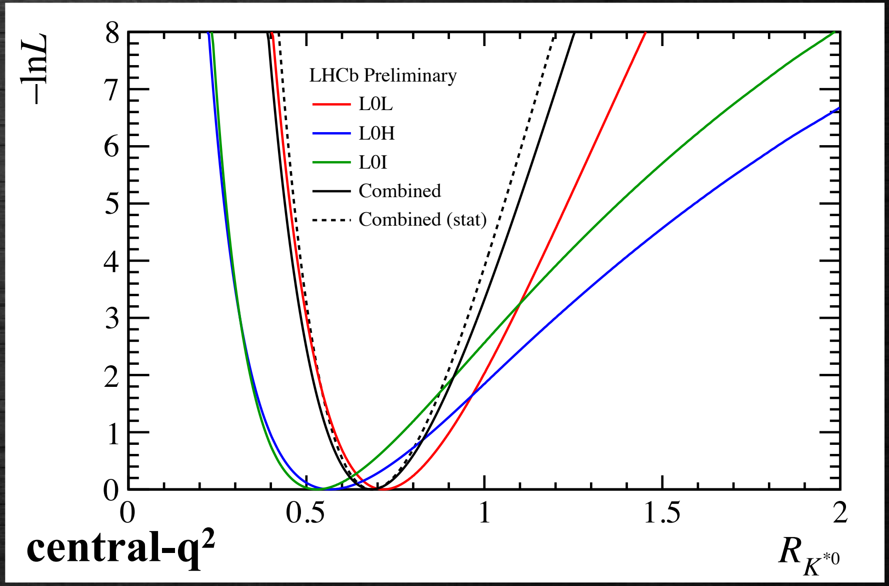

› The measured values of $R_{K^{*0}}$ are found to be in good agreement among the three trigger categories in both q^2 regions

Results – II

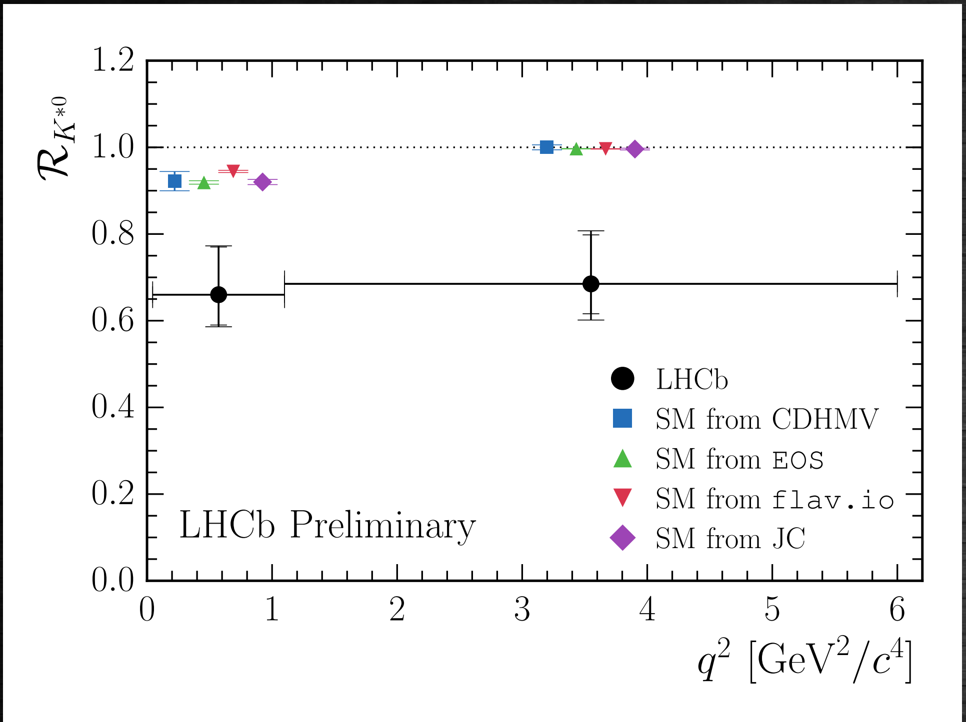

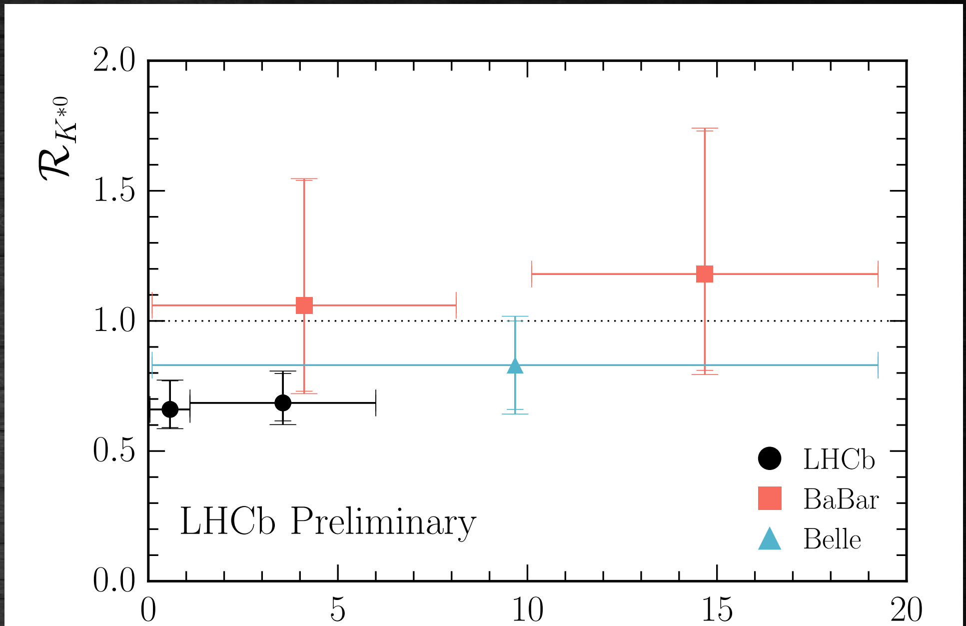

- PRD 86 (2012) 032012
- PRL 103 (2009) 171801

› The compatibility of the result in the **low-q^2** with respect to the SM prediction(s) is of **2.2-2.4** standard deviations

› The compatibility of the result in the **central-q^2** with respect to the SM prediction(s) is of **2.4-2.5** standard deviations

Summary and Outlook

- Using the full Run 1 data set the $R_{K^{*0}}$ ratio has been measured by LHCb with the best precision to date in two q^2 bins
- The compatibility of the result with respect to the SM prediction(s) is of 2.2-2.5 standard deviations in each q^2 bin
- The result is particularly interesting given a similar behaviour in R_K
- Rare decays will largely benefit from the increase of energy (cross-section) and collected data (~5 fb^{-1} expected in LHCb) in Run 2
- LHCb has a wide programme of LU tests based on similar ratios
- Future measurements will be able to clarify whether the tantalising hints we are observing are a glimpse of NP

Backup

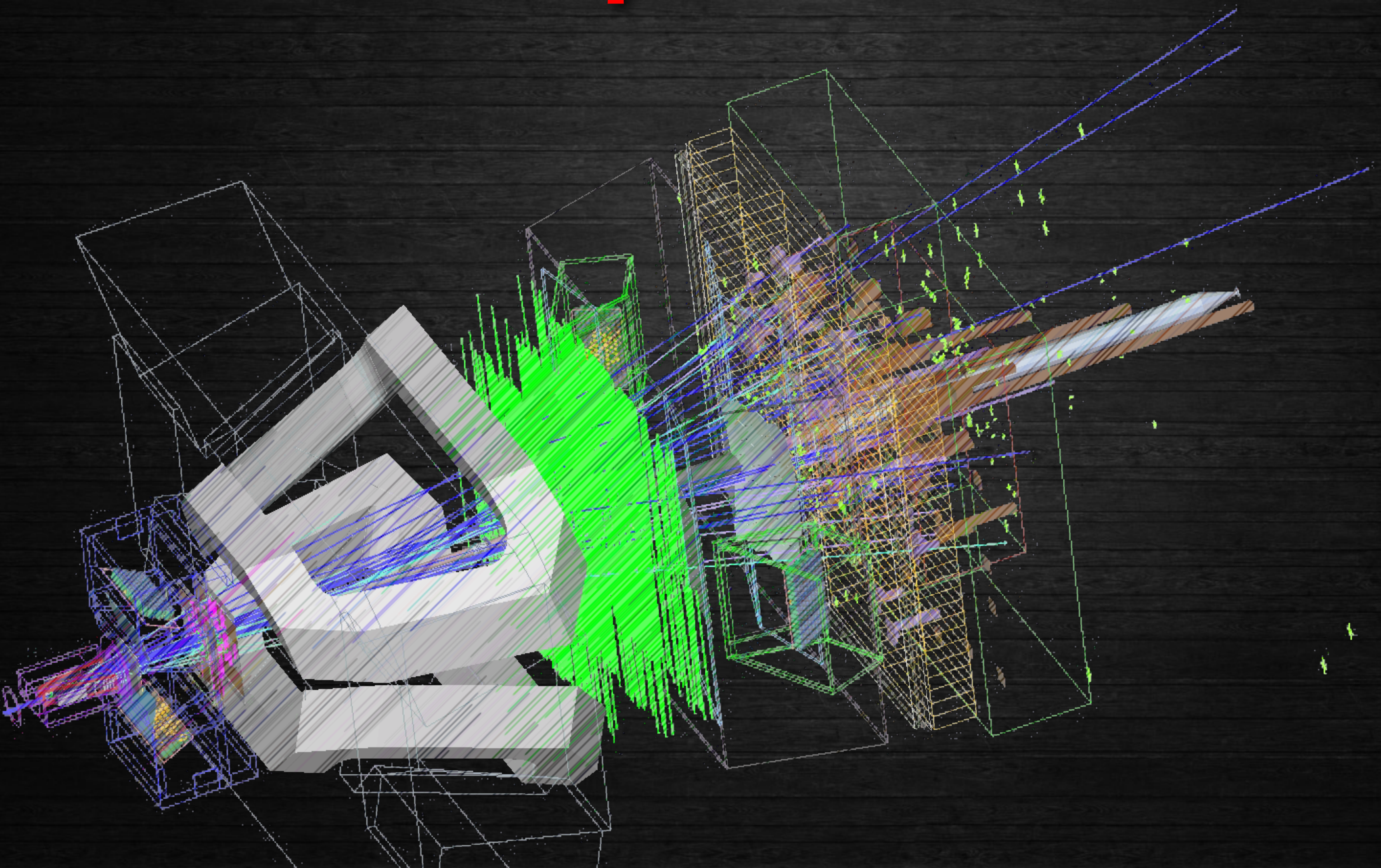

Calorimeter System

› Composed of a Scintillating Pad Detector (SPD), a Preshower (PS), an electromagnetic calorimeter (ECAL) and a hadronic calorimeter (HCAL)

› The SPD and the PS consist of a plane of scintillator tiles (2.5 radiation lengths, but to only ~6% hadronic interaction lengths)

› The ECAL has shashlik-type construction, i.e. a stack of alternating slices of lead absorber and scintillator (25 radiation lengths)

› The HCAL is a sampling device made from iron and scintillator tiles being orientated parallel to the beam axis (5.6 interaction lengths)

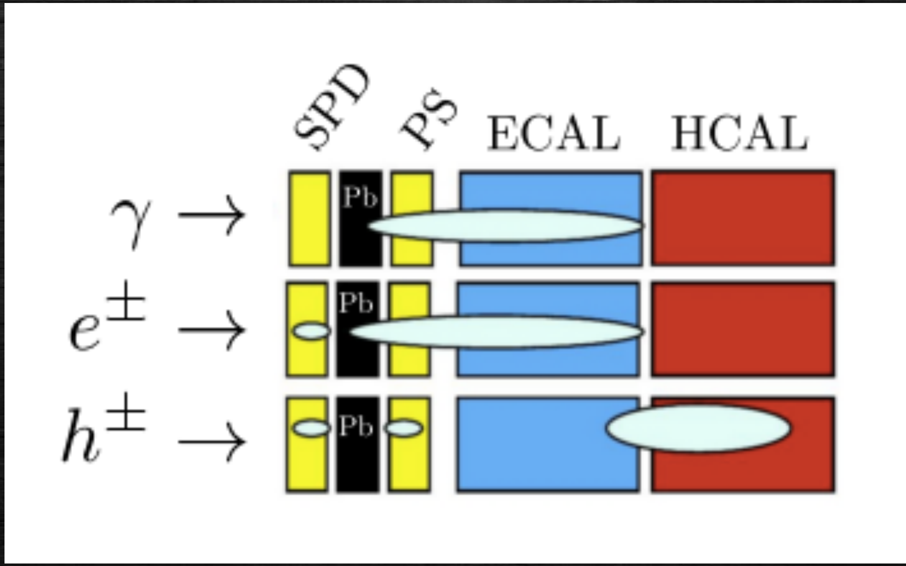

Cross-Checks – III

› Relative population of **bremsstrahlung categories** compared between data and simulation using $B^0 \to K^{*0} J/\psi(ee)$ and $B^0 \to K^{*0}\gamma(ee)$ events

Table 6: Fraction of simulated $B^0 \to K^{*0} J/\psi\,(\to e^+e^-)$ and $B^0 \to K^{*0}\gamma(\to e^+e^-)$ events (in percent) with 0, 1 and 2 recovered photons per trigger category. The number in brackets is determined on data. For $B^0 \to K^{*0}\gamma(\to e^+e^-)$, due to the very low opening angle of the two electrons, it is not possible to assign unambiguously one photon to a track.

Trigger category	$\mathbf{0\gamma}$	$\mathbf{1\gamma}$	$\mathbf{2\gamma}$
	$\boldsymbol{B^0 \to K^{*0} J/\psi\,(\to e^+e^-)}$		
L0E	27.7 ± 0.2 (26.6 ± 0.2)	49.7 ± 0.2 (50.0 ± 0.2)	22.6 ± 0.2 (23.4 ± 0.2)
L0H	16.7 ± 0.6 (15.1 ± 0.6)	49.5 ± 0.8 (50.4 ± 0.8)	33.8 ± 0.8 (34.6 ± 0.7)
L0I	22.4 ± 0.4 (21.4 ± 0.4)	50.2 ± 0.5 (50.4 ± 0.5)	27.2 ± 0.4 (28.3 ± 0.4)
	$\boldsymbol{B^0 \to K^{*0}\gamma(\to e^+e^-)}$		
L0E	34.9 ± 2.4 (33.2 ± 2.8)	65.1 ± 2.4 (66.8 ± 2.8)	–
L0H	28.2 ± 3.4 (28.8 ± 4.1)	71.8 ± 3.4 (71.2 ± 4.1)	–
L0I	32.9 ± 3.0 (32.4 ± 3.2)	67.1 ± 3.0 (67.6 ± 3.2)	–

› A good agreement is observed

Cross-Checks – VII

› The distance between the Kπ and ll vertices

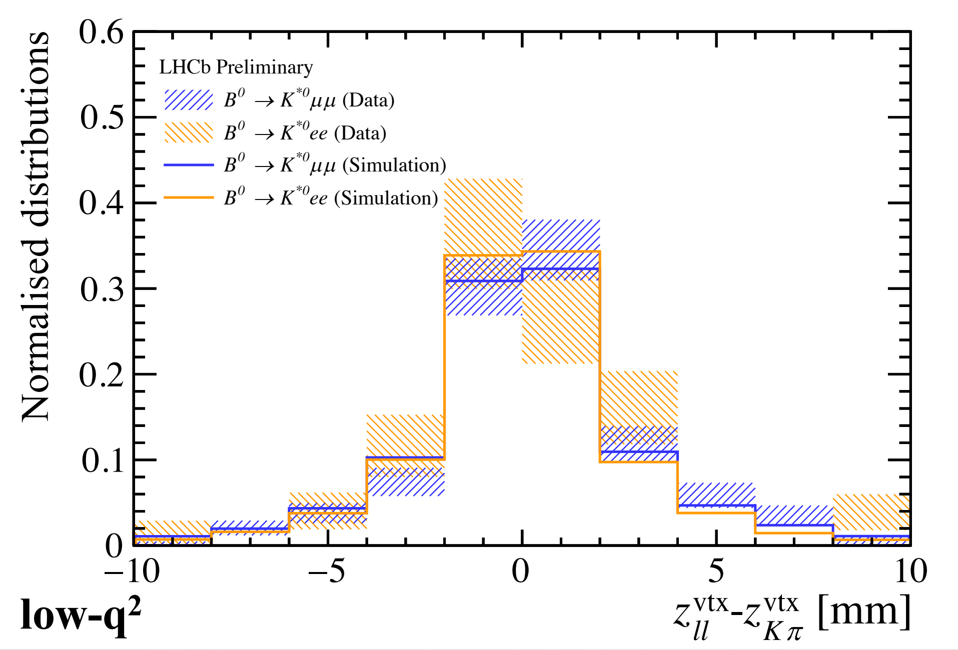

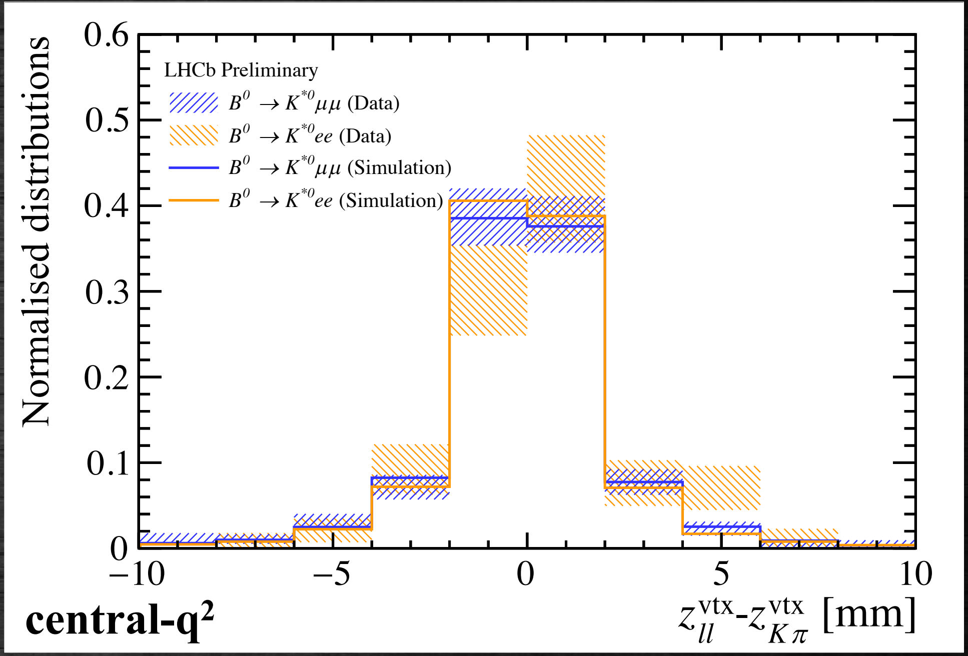

› The hadron and lepton pairs consistently originate from the same decay vertex

Results – III

› What about NP?

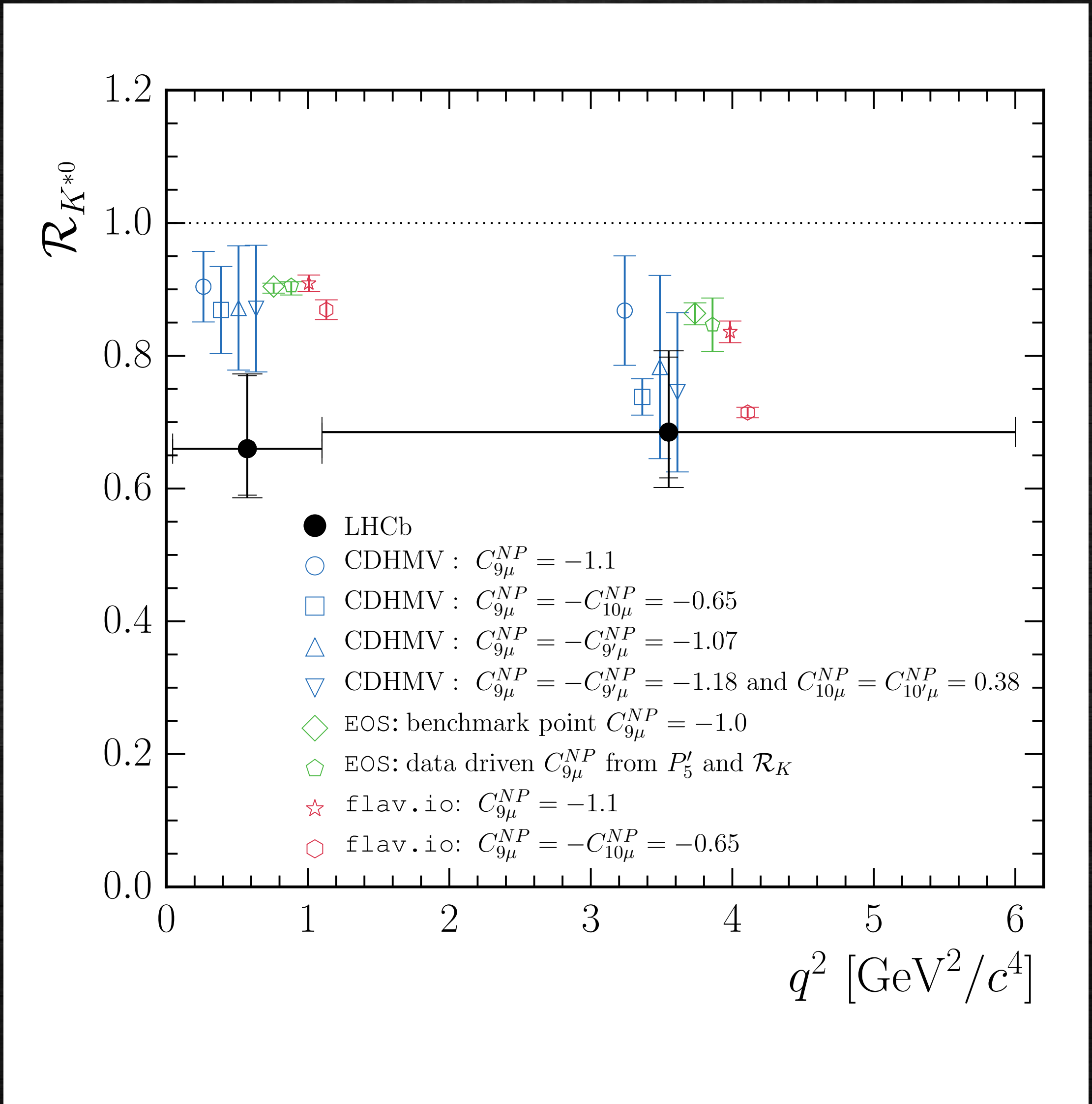

Di-Lepton Mass

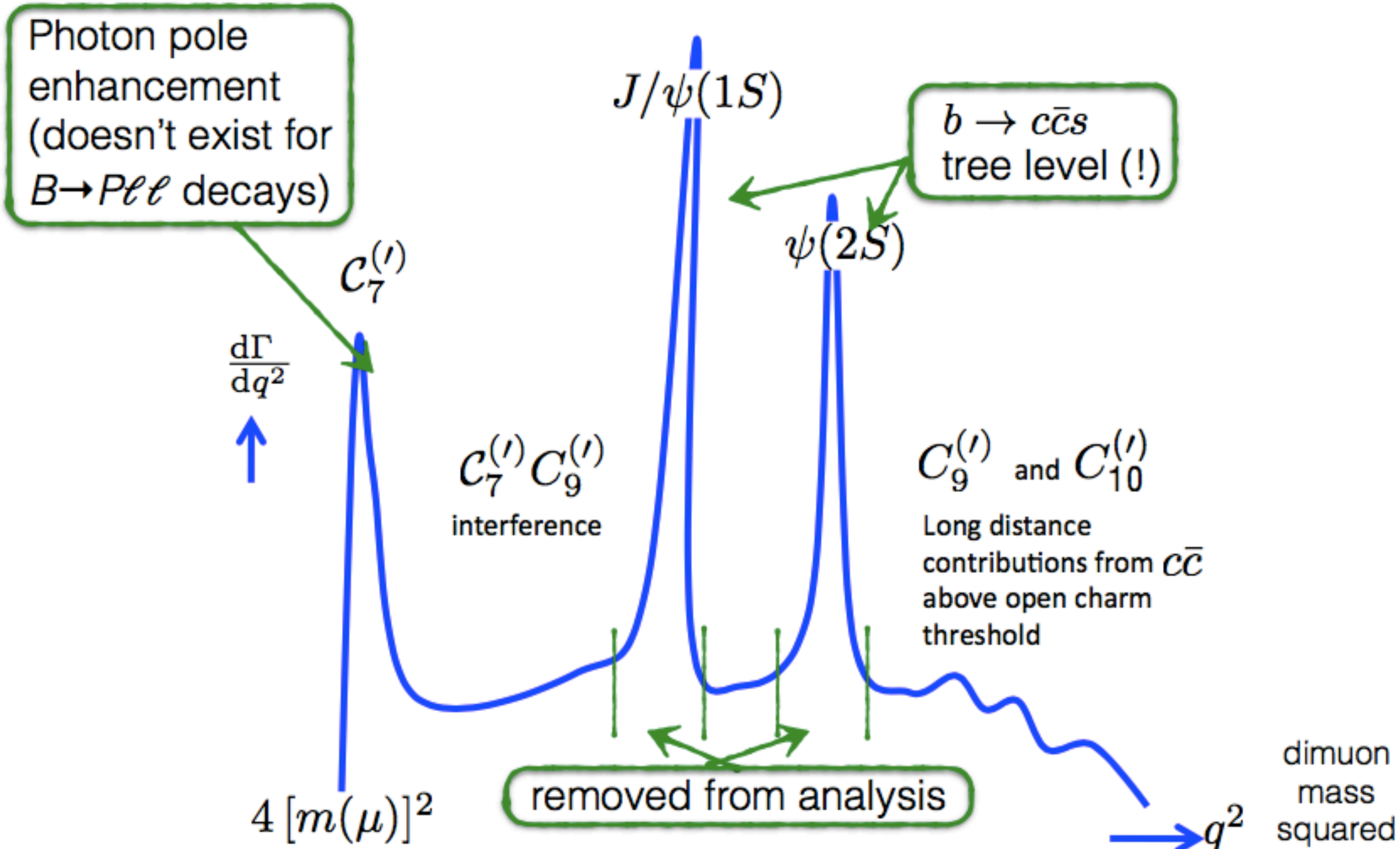

Theoretical Framework

- In the Fermi model of the weak interaction, the full electroweak Lagrangian (which was unknown at the time) is replaced by the low-energy theory (QED) plus a single operator with an effective coupling constant.

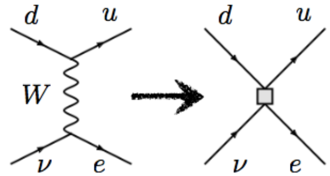

$$\mathcal{L}_{\mathrm{EW}} \to \mathcal{L}_{\mathrm{QED}} + \frac{G_{\mathrm{F}}}{\sqrt{2}}(\overline{u}d)(e\overline{\nu})$$

- Can write a Hamiltonian for the effective theory as

$$\mathcal{H}_{\mathrm{eff}} = -\frac{4\,G_F}{\sqrt{2}} V_{tb} V_{ts}^{*} \frac{\alpha_e}{4\pi} \sum_i C_i(\mu)\, \mathcal{O}_i(\mu),$$

Wilson coefficient (integrating out scales above μ)

Local operator with different Lorentz structure (vector, axial vector current etc)

Operators

SM operators

photon penguin

$$\mathcal{O}_7 = \frac{m_b}{e}\bar{s}\sigma^{\mu\nu}P_R b F_{\mu\nu}\,,$$

$$\mathcal{O}_8 = g_s\frac{m_b}{e^2}\bar{s}\sigma^{\mu\nu}P_R T^a b G^a_{\mu\nu}\,,$$

$$\mathcal{O}_9 = \bar{s}\gamma_\mu P_L b\,\bar{\ell}\gamma^\mu\ell\,,$$

$$\mathcal{O}_{10} = \bar{s}\gamma_\mu P_L b\,\bar{\ell}\gamma^\mu\gamma_5\ell\,,$$

vector and axial-vector currents

Beyond SM operators

$$\mathcal{O}'_7 = \frac{m_b}{e}\bar{s}\sigma^{\mu\nu}P_L b F_{\mu\nu}\,,$$

$$\mathcal{O}'_8 = g_s\frac{m_b}{e^2}\bar{s}\sigma^{\mu\nu}P_L T^a b G^a_{\mu\nu}\,,$$

$$\mathcal{O}'_9 = \bar{s}\gamma_\mu P_R b\,\bar{\ell}\gamma^\mu\ell\,,$$

$$\mathcal{O}'_{10} = \bar{s}\gamma_\mu P_R b\,\bar{\ell}\gamma^\mu\gamma_5\ell\,.$$

right handed currents (suppressed in SM)

Angular Analyses

- Complex angular distribution:

$$
\frac{1}{\mathrm{d}(\Gamma+\bar{\Gamma})/\mathrm{d}q^2}\frac{\mathrm{d}^3(\Gamma+\bar{\Gamma})}{\mathrm{d}\vec{\Omega}}\bigg|_{\mathrm{P}} = \frac{9}{32\pi}\Big[\tfrac{3}{4}(1-\boxed{F_{\mathrm{L}}})\sin^2\theta_K + \boxed{F_{\mathrm{L}}}\cos^2\theta_K +
+\tfrac{1}{4}(1-\boxed{F_{\mathrm{L}}})\sin^2\theta_K\cos2\theta_l
-\boxed{F_{\mathrm{L}}}\cos^2\theta_K\cos2\theta_l + S_3\sin^2\theta_K\sin^2\theta_l\cos2\phi
+S_4\sin2\theta_K\sin2\theta_l\cos\phi + \boxed{S_5}\sin2\theta_K\sin\theta_l\cos\phi
+\tfrac{4}{3}\boxed{A_{\mathrm{FB}}}\sin^2\theta_K\cos\theta_l + S_7\sin2\theta_K\sin\theta_l\sin\phi
+S_8\sin2\theta_K\sin2\theta_l\sin\phi + S_9\sin^2\theta_K\sin^2\theta_l\sin2\phi\Big]
$$

fraction of longitudinal polarisation of the K*

forward-backward asymmetry of the dilepton system

The observables depend on form-factors for the $B \to K^*$ transition plus the underlying short distance physics (Wilson coefficients).

Interpretation of Global Fits

Optimist's view point

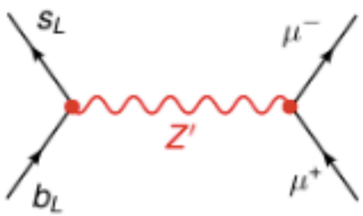

Vector-like contribution could come from new tree level contribution from a Z' with a mass of a few TeV

Pessimist's view point

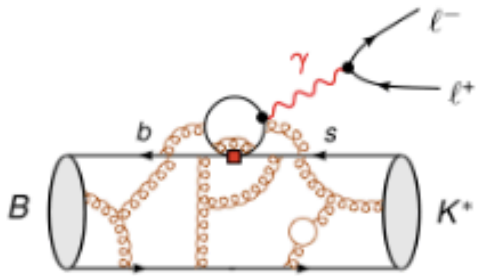

Vector-like contribution could point to a problem with our understanding of QCD, e.g. are we correctly estimating the contribution for charm loops that produce dimuon pairs via a virtual photon.

More work needed from experiment/theory to disentangle the two

Interpretation of Global Fits

- This is the physics we are interested in.

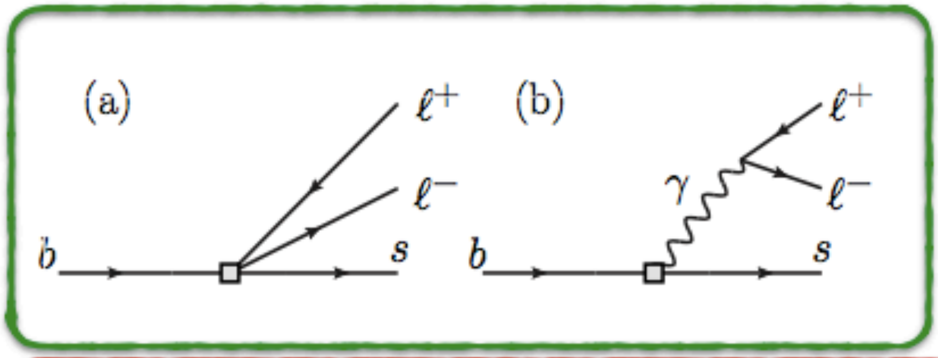

■ Short distance part integrates out (as a Wilson coefficient)

- We also get long-distance hadronic contributions. Included in the SM but are the predictions correct?